CHAPTER 10

ORE MINERAL ASSEMBLAGES OCCURRING IN SEDIMENTARY, VOLCANIC, METAMORPHIC, AND EXTRATERRESTRIAL ENVIRONMENTS

10.1 INTRODUCTION

In this chapter, the discussion of characteristic associations is continued and extended to ores occupying a variety of sedimentary, volcanic, and metamorphic environments. It concludes with a brief account of the occurrence of ore minerals in meteorites and lunar rocks. As in Chapter 9, the common associations are described, and their modes of origin are briefly discussed. Again, no attempt is made to give a comprehensive account of their geology and petrology.

The first associations described represent part of the continuum of sedimentary processes and include placer-type titanium, tin, and gold deposits, chemical precipitates, coal, and base-metal accumulations that are spatially related to submarine hydrothermal vents and volcanism. Lead-zinc deposits in carbonates (and arenites), although normally regarded as epigenetic, are included here because of their stratabound nature and the increasingly prevalent belief that they are related to diagenetic processes and to the migration of connate brines. The effects of regional metamorphism on ores, especially massive sulfides of sedimentary-volcanic affiliation, are treated in Section 10.10, and the contact metamorphic skarn deposits are discussed in Section 10.11. The unique mineralogical characteristics of extraterrestrial materials, which are becoming increasingly available for study, are described in Section 10.12. References are given to the relevant literature at the end of each section; many additional articles appear regularly in such major periodicals as *Economic Geology, Mineralium Deposita, Transactions of the Institution of Mining and Metallurgy, The Canadian Mineralogist,* and *Ore Deposit Reviews.*

10.2 IRON AND MANGANESE ORES IN SEDIMENTARY ENVIRONMENTS

10.2.1 Iron

Most sedimentary rocks contain significant quantities of iron, and there is a complete range up to those of ore grade. Sedimentary iron ores can broadly be considered as occurring in three major classes: bog iron ores, ironstones, and (banded) iron formations. This also is the increasing order of their economic importance.

Bog Iron Ores

Mineralogy Goethite, limonite, siderite; minor carbonates, vivianite [$Fe_3(PO_4)_2{\cdot}8H_2O$].

Mode of Occurrence As lake or swamp sediments, often in temperate or recently glaciated areas or in volcanic streams and lakes; also in association with coal measures in older sedimentary sequences ("blackband ironstones").

Examples In tundra areas of Canada and Scandinavia; temperate coastal areas of the eastern United States and Canada; in volcanic provinces such as Japan and the Kurile Islands; in carboniferous and Permian sedimentary sequences in the eastern United States and Northern England.

Mineral Associations and Textures Goethite, the major phase of many bog iron deposits, occurs as oolitic or pisolitic grains (1–10 mm) cemented to form disks (~3–30 cm diameter), which, in turn, form bands or lenses of ore. The ores also commonly occur as colloform bands and irregular module-like masses that are composed of mm-to-cm-length radiating fibrous crystals of goethite. Other examples are comprised of more earthy limonite material with substantial carbonate and phosphate. The blackband ironstones are largely siderite.

Ironstones

Mineralogy Chamosite $(Fe,Al)_6(Si,Al)_4O_{10}(OH)_8$, hematite, limonite or goethite, siderite; minor magnetite, pyrite, collophane $Ca_5(PO_4)_3$, greenalite [$Fe^{2+},Fe^{3+})_6Si_4O_{10}(OH)_8$].

Mode of Occurrence As the "minette-type" (or Clinton-type) ores deposited in shallow-water marine sequences that are associated with a variety of sedimentary rocks, including limestones, siltstones, shales, and sandstones. Also, to a minor extent, they occur in volcanic sediments.

Examples Minette- or Clinton-type ores occur in Phanerozoic sediments of the Jurassic Age in Alsace-Lorraine and other areas of France, Germany, Belgium, and Luxembourg; in the Jurassic of England and in the Silurian (Clinton Beds) of the United States; in volcanic sediments, Lahn-Dill, Germany.

Mineral Associations and Textures Megascopically, ironstones appear as dull, reddish earthy sandstones or as oolitic or pelletal accumulations that may be distinctly green or red-brown in color. Microscopically, they appear as oolitic, pisolitic, or pelletal grains that may have been entirely or partially replaced by interlayered limonite and hematite (Figure 10.1). As in modern sediments, most ooids and pellets have formed around sand grains or fragmental fossil or mineral material. Micro- and macrofossils are commonly present and may also be replaced by iron minerals. Siderite may occur, chiefly as cementing material, and the silicate, oxide, and carbonate may occur in a wide range of ratios and detailed textural relationships. In sand facies, the iron minerals occur dominantly as concentric quartz grain coatings and interstitial filling.

Banded Iron Formations

Mineralogy Major hematite and magnetite, and in some cases iron carbonates and silicates may be important; pyrite usually minor. Major gangue mineral is chert.

Mode of Occurrence As well-bedded, elongate bodies, often with alternating chert-iron mineral stratification. The ores occur as laterally and vertically extensive sequences in Precambrian strata throughout the world. In some cases, the sedimentary setting appears to have been marine; in others, estuarine or fresh water; and sometimes an association with volcanic rocks is evident.

Examples Widespread in Precambrian sequences, but major examples include the Lake Superior district of Minnesota-Wisconsin-Michigan-Ontario-Quebec and the Labrador-Quebec belts of North America, the Hamersley Basin of Western Australia, and deposits in Brazil, India, and South Africa.

Mineral Associations and Textures Characterized by banding resulting from the interlayering of oxides and silica, both on a coarse and a fine scale (see Figure 10.2); the units may be lenses rather than layers, giving a "wavy" appearance to the stratification. Hematite and magnetite constitute the major ore minerals, but iron in carbonate, silicates (greenalite, minnesotaite, stilpnomelane), and sulfides (pyrite and very minor pyrrhotite) is also found. In the classic work of James (1954, 1966), the occurrence of the ores dominantly as oxide, carbonate, silicate, or sulfide has been related to a chemical "facies" of

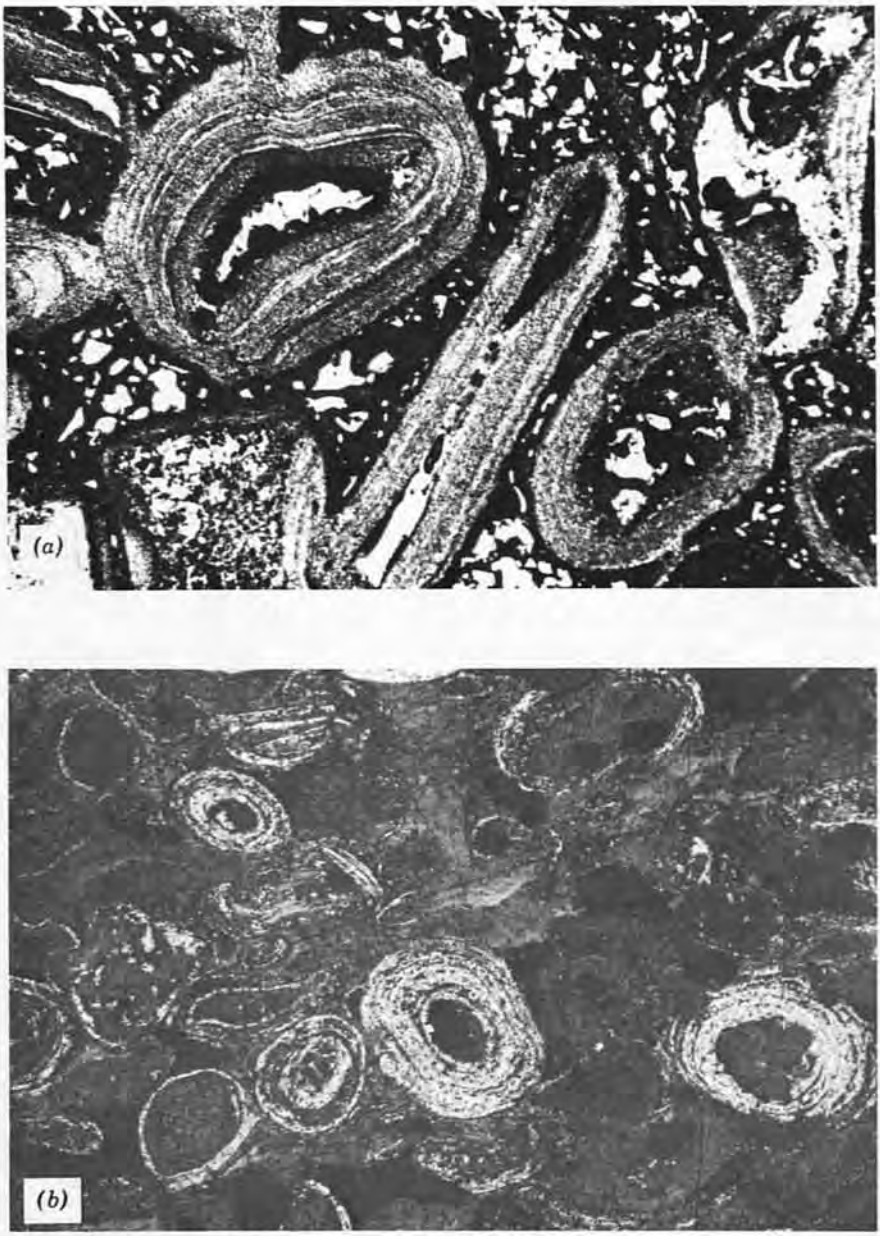

FIGURE 10.1 Textures observed in typical ironstones. (*a*) Distorted ooliths comprised of fine-grained chamosite, hematite, and goethite, Red Mountain Formation, Alabama (width of field = 2,000 μm). (*b*) Ooliths of chamosite and goethite, Rosedale, Northern England (width of field = 2,000 mm).

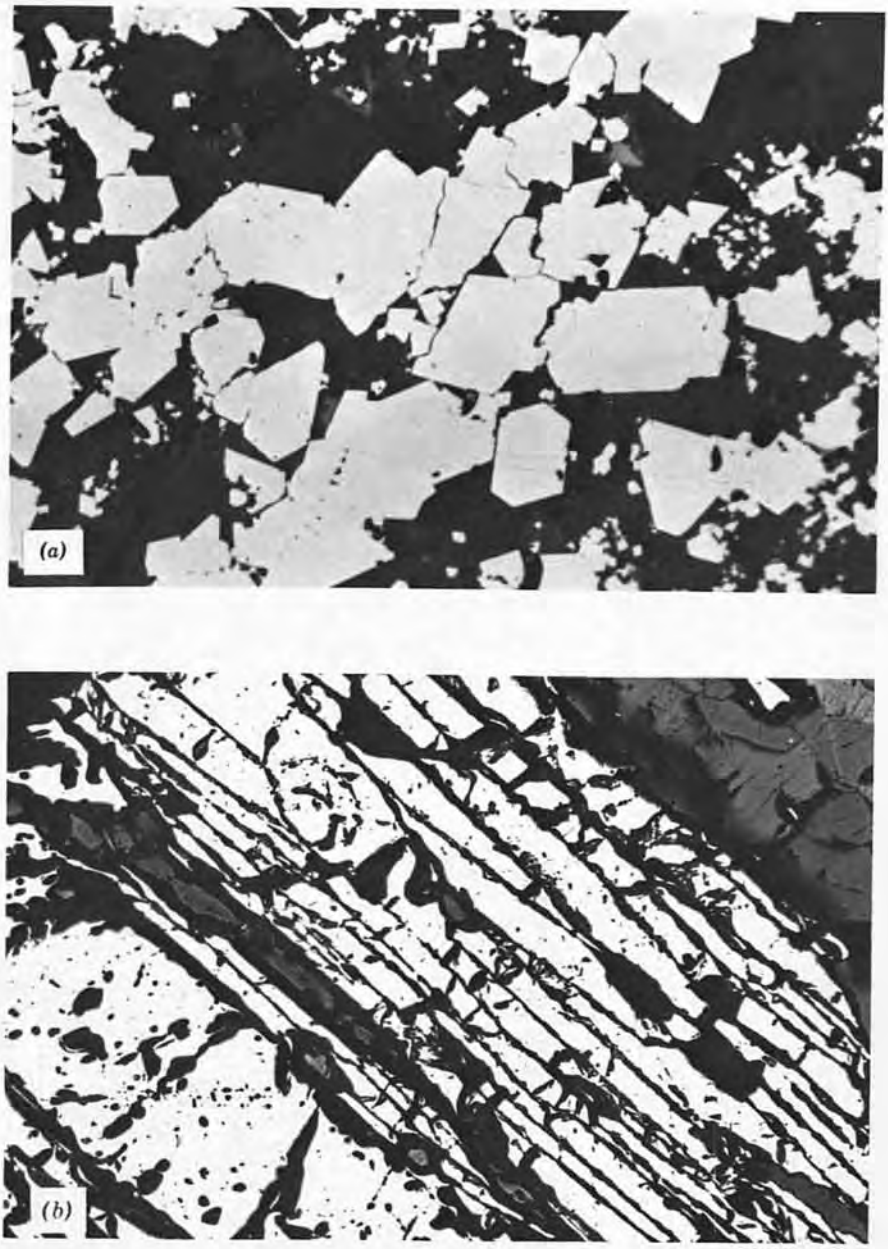

FIGURE 10.2 Typical banded iron formation assemblages and textures. (*a*) Layered subhedral magnetite, Eastern Gogebic Range, Michigan (width of field = 300 μm). (*b*) Bladed specular hematite with blocky magnetite, Rana Gruber Mines, Norway (width of field = 2,000 μm).

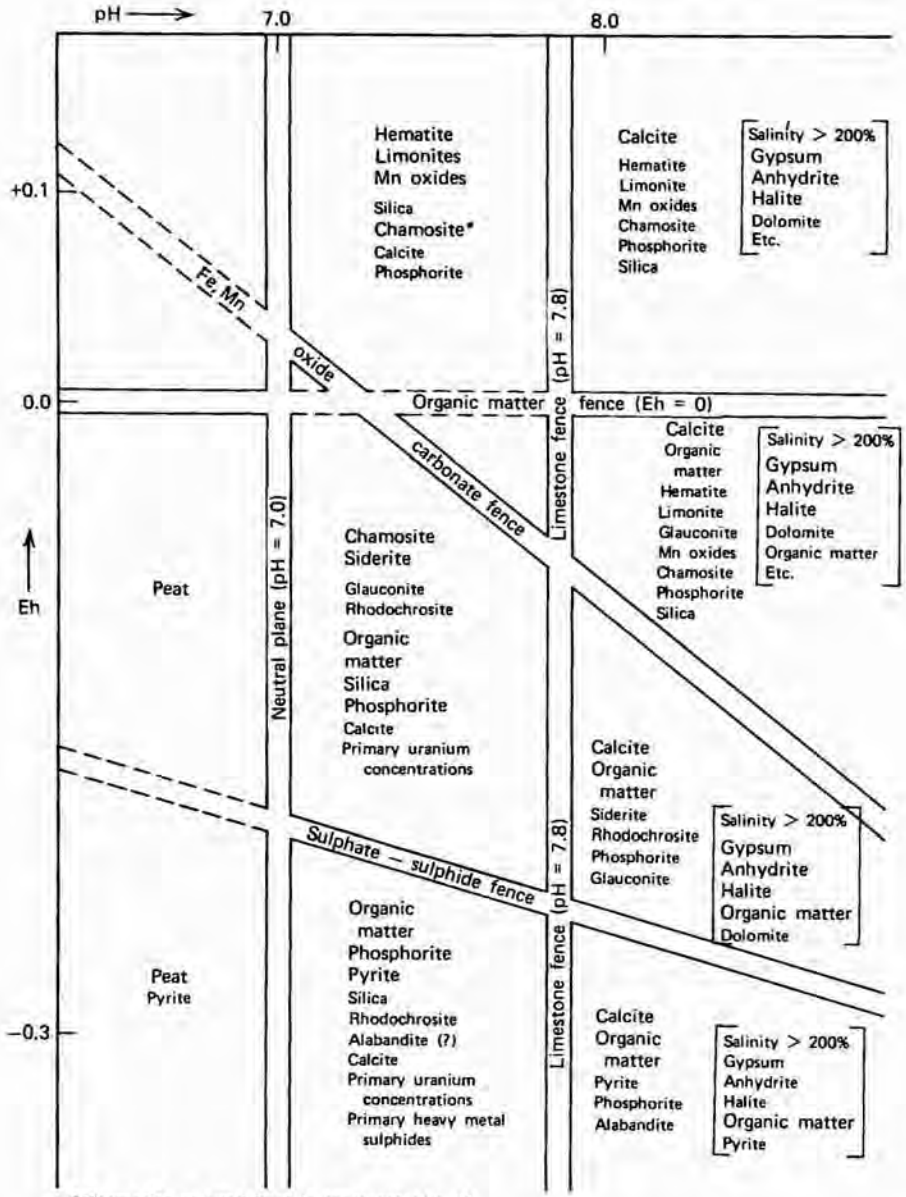

FIGURE 10.3 Fence diagram showing Eh-pH fields in which end member minerals important in sedimentary iron ores and other chemical sediments are formed under normal seawater conditions. Associations in brackets are for hypersaline conditions (salinity >200%). (Reprinted from W. C. Krumbein and R. M. Garrels, "Origin and Classification of Chemical Sediments in Terms of pH and Oxidation-Reduction Potential," *Jour. Geol.* **60**, 26, 1952, by permission of the University of Chicago Press.)

precipitation dependent on Eh and pH conditions, as indicated in Figure 10.3.

In the oxide facies, two major variants occur—a banded hematite/chert ore and a banded magnetite/chert ore. In the former category, the hematite may occur in the form of ooliths or pisoliths, as finely crystalline laminae, or as laths oriented subparallel to the bedding (Figure 10.2b). The latter subdivision shows more variation, with carbonate and silicate phases often present. Magnetite occurs as disseminated to massive bands of subhedral to euhedral grains (Figure 10.2a). The carbonate facies has interlayered chert and carbonate that may grade into interlayered silicate/magnetite/chert or carbonate/pyrite. The sulfide facies is characteristically associated not with chert, but with black carbonaceous shales in which the sulfide is normally very fine pyrite having clear crystal outlines. Any pyrrhotite is normally found as fine plates, with the long axis parallel to bedding. The silicate facies can occur in association with any of the other facies type.

10.2.2 Origins of Iron-Rich Sediments

The bog iron ores can be observed in the process of formation, so their origin is clearly understood. In the closed drainage systems in tundra areas, these ores are derived by subsurface weathering and leaching, with transport of the iron as bicarbonates and humates in ground water of low pH and Eh, and subsequent concentration and deposition in lakes and marshes by loss of CO_2 and, commonly, oxidation. The origin of blackband ores is less certain; some may be primary, and others may be of diagenetic origin.

The origins of *ironstone* deposits pose major problems regarding both the source of the iron and the methods by which it is concentrated (see Young and Taylor, 1989, for further discussion). In particular cases, the ultimate source of iron may have been continental erosion, submarine volcanic springs, or upwelling ocean currents. The site of final deposition was commonly a shallow water marine environment, but, since this was a relatively high-energy, oxygenated environment, formation of chamosite is unlikely to have occurred here. Possibly the initial formation of chamosite occurred in a reducing environment beneath the sediment surface, with subsequent transport to the site of accumulation. Ooid formation may have occurred diagenetically during initial formation or during the processes of transport and final deposition. Any understanding of the origin of these ores is further hindered by their complex diagenetic history, which often involves total or partial replacement of ooliths and fossil fragments. These replacement features have led to suggestions that the ores result from wholesale replacement of oolitic limestones by iron minerals, but detailed study of the textures and geological settings shows many flaws in this model.

The banded iron formations are very different from the ironstones, in that the former have very low contents of Al_2O_3 and P_2O_5 and a high silica (chert) content. Their restriction to the Precambrian (and Cambrian) is also con-

sidered significant in some theories and requires explanation, as does the regular interbedding of iron ore and chert. Various theories have proposed cyclical continental erosion, seaboard and submarine volcanism, or seafloor leaching as the origin of the iron, with deposition in either a marine or a lacustrine environment. Many workers believe that the absence of free oxygen in the early to mid-Precambrian atmosphere was an important factor in the transport and precipitation of the iron. There is, however, no consensus of opinion regarding the mechanisms of formation. For the arguments in favor and against various conflicting theories, the reader is referred to the standard texts on ore geology and to *Economic Geology*, Vol. 68, No. 7 (1973), "Precambrian Iron Formations of the World" or the other original papers.

10.2.3 Manganese

Most sedimentary rocks also contain detectable concentrations of manganese, although, generally, this is an order of magnitude lower in concentration than iron; as with iron-rich sediments, there is a complete range from minor amounts to ore grades. The major classes of sedimentary manganese ores are marsh and lake deposits, deposits of the orthoquartzite-glauconite-clay association, deposits of volcanic affiliation, and modern marine deposits (including *manganese nodules*). The marsh and lake deposits are commercially insignificant and are undoubtedly the analogues of bog iron ores, being derived by the same processes. The manganese occurs as poorly crystalline hydrous oxides. The other classes of sedimentary manganese deposits will be briefly discussed in turn.

10.2.4 Manganese Deposits of Orthoquartzite-Glauconite-Clay Association

Mineralogy Pyrolusite, psilomelane, manganite, manganocalcite, and rhodochrosite ($MnCO_3$).

Mode of Occurrence Thin lens-shaped beds conformable with enclosing sedimentary strata, the sediments having generally been deposited on a stable platform area and being estuarine through to shallow marine deposits (sandstones, silts, clays, glauconitic beds, limestones, and even coaly beds).

Examples Southern Soviet Union (Nikopol, Chiatura, etc.); Timna region of Southern Israel; Turkey and Bulgaria and other localities of the Northern Mediterranean (all in Tertiary strata); Northern Australia (L. Cretaceous beds of Groote Eylandt).

Mineral Associations and Textures The mineral associations and their spatial relationships appear to reflect different facies of chemical sedimentation, as suggested for certain iron deposits; in this case, a sequence of oxide,

oxide-carbonate, carbonate ore appears to represent successively greater distance from a palaeo-shoreline. The ores generally consist of irregular concretions and nodules and earthy masses of the oxides or carbonates in a silt or clay matrix (see Figure 10.4a).

10.2.5 Manganese Deposits of the Limestone-Dolomite Association

Mineralogy Dominantly either oxides (pyrolusite, hausmannite, bixbyite, psilomelane, etc.) in type 1 or carbonate (rhodochrosite, etc.) in type 2 (see below).

Mode of Occurrence Subdivided by Varentsov (1964) into:

1. Manganiferous limestone—dolomite formations developed on stable platforms ("Moroccan type")
2. Manganiferous limestone—dolomite formations of geosynclinal zones ("Appalachian-type" and "Usinsk type")

Type 1 consists of a sequence of manganese oxide ores interlayered with dolomites, limestones, and sometimes gypsum, with both underlying and overlying red terrigenous sediments, all deposited on the eroded surface of a stable platform. Type 2 consists either merely of manganiferous limestone or more complex manganese carbonate ores in limestone-dolomite sequences associated with volcanic deposit.

Examples North Africa (Morocco), Appalachian area (United States), Usinsk deposit (S.W. Siberia, Russia).

Mineral Associations and Textures In both types of deposits, the ore zones vary from small lenses to continuous beds of Mn-rich sediment. The associations of type 1 are composed almost entirely of oxides and are low in iron, aluminum, and phosphorus, although heavy metal impurities are characteristic (BaO < 7%, PbO < 6.5%). The ores of type 2 are dominated by calcian and ferroan rhodocrosites and also make up >8% of the rock. The carbonates occur as ooliths and very fine laminae intercalated with manganoan stilpnomelane. Algal and sponge remains commonly occur, and may be replaced by Mn carbonate. The type 2 ores, although low in Ba and Pb, may contain >15% iron oxide and minor phosphorus.

10.2.6 Manganese Deposits of Volcanic Affiliation

Mineralogy Dominantly, the manganese oxides (hausmannite, jacobsite, etc.). Also braunite and associated iron oxides (hematite, magnetite) and minor sulfides (pyrite, arsenopyrite, chalcopyrite, galena, sphalerite, tetrahedrite); also quartz and chalcedony.

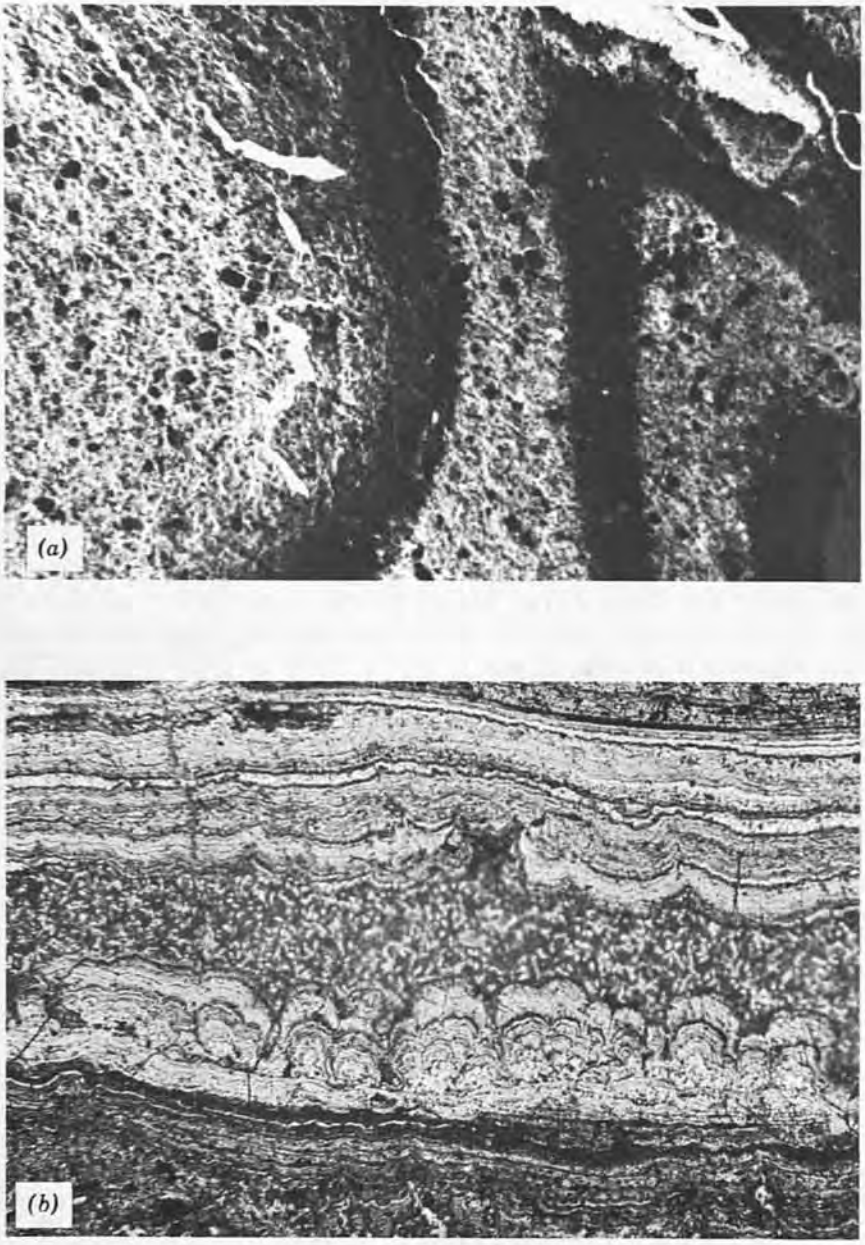

FIGURE 10.4 Manganese ores. (*a*) Psilomelane showing characteristic growth texture (width of field = 2,000 μm). (*b*) Textures of a characteristic manganese nodule, Blake Plateau, Atlantic Ocean (width of field = 520 μm).

Mode of Occurrence Very widespread in volcanic-sedimentary sequences as concordant lenses of ore (generally rather small).

Examples In Palaeozoic pyroclastic sequences in Western North America, the Urals (Russia), East Australia; in Tertiary volcanic sequences in Japan, Indonesia, and the West Indies.

Mineral Associations and Textures The manganese occurs as layered and colloform to botryoidal masses of intermixed pyrolusite, psilomelane, todorokite, and jacobsite. Grain size varies from the micron scale to radiating fibrous masses in which the fibers exceed 1 cm in length.

10.2.7 Modern Marine Deposits ("Manganese Nodules")

Mineralogy In manganese nodules and marine ferromanganese crusts, the dominant minerals are Mn^{4+} oxides related to the terrestrial minerals todorokite, δ-MnO_2 (sometimes termed *vernadite*), or, more rarely, birnessite. Although most nodules contain significant concentrations of iron, the iron-bearing phases in most nodules are poorly crystalline; recently, the mineral feroxyhyte (δ'-FeOOH) has been claimed to occur as a precursor to goethite (α-FeOOH). Common minor phases are goethite, quartz, feldspar, clays, and zeolites. Manganese-rich sediments and oozes have been less well studied but are also dominated by fine-grained oxide and hydroxide phases.

Mode of Occurrence Manganese nodules are widely distributed on the floors of the major oceans and are generally spherical and 1–30 cm in diameter (Cronan, 1992). Their importance as a resource is related not only to the manganese and iron they contain, but also to the presence of significant cobalt, nickel, and copper taken up within the structures of the manganese minerals (see Section 11.4.5). Manganese-rich sediments and oozes also occur in ocean regions with a clear link to submarine volcanism in some cases; they also occur in confined seas as those of the arctic regions.

Mineral Associations and Textures The internal structure of manganese nodules is of porous concentric, often colloform, zoning, with layering of different widths clearly visible under the microscope (see Figure 10.4b). The zones have been classified as laminated, massive, columnar, compact, and mottled, and contain simple, arcuate, or chaotic layering (Sorem and Foster, 1972). The zones of high reflectance are those rich in Mn and containing Ni and Co; the darker bands are Fe-rich. The porosity, fractures, irregular layering, and included organic matter require impregnation of materials prior to preparation of polished sections.

10.2.8 Origins of Manganese-Rich Sediments

The manganese deposits of volcanic affiliation almost certainly owe their origin to direct discharge of manganese from submarine volcanoes or hot springs and subsequent accumulation as chemical sediments, along with other sedimentary and volcanic detritus. A similar origin can be invoked for certain manganese concentrations in modern marine environments.

In contrast, the manganese ores of limestone-dolomite and of ortho-quartzite-glauconite-clay association show no clear indication of a volcanic origin for the manganese, although this has been invoked by some authors. Both the source of manganese and the mechanism of its precipitation are more problematic.

The origin of the manganese and other metals concentrated in nodules and oozes may derive from volcanic and partly from terrigenous sources. The growth of nodules apparently takes place by the release of ions in the reducing environment beneath the sediment surface, their upward migration when thus mobilized, and their subsequent fixation following oxidation at the sediment surface and attachment as layers on a detrital particle (Glasby, 1977; Burns, 1979).

10.2.9 Gossans

General Gossans, or "iron caps," develop on many types of iron-sulfide-bearing deposits as a result of surface or near-surface weathering and oxidation.

Mineralogy Goethite, limonite, lepidocrocite, hematite in varying proportions, sometimes with minor amounts of manganese oxides and residual base-metal sulfides and, locally, trace quantities of gold.

Examples Developed worldwide at surficial exposures of sulfide-containing deposits.

Mineral Associations and Textures Gossans generally consist of porous irregular laminae and colloform bands of mixed iron oxides with minor, but variable, amounts of residual sulfide minerals. Remnant textures or primary grain shapes, cleavages, and fractures are commonly preserved in the iron oxides. The grain size is usually very fine (< 10 μm), but radiating bundles of fibrous crystals (like those in Figure 7.13) up to 1 millimeter or more in length may be locally developed. In recent years, several gossans have been mined for gold that was dissolved from the primary ores and reprecipitated during the gossan-forming process.

Origin of Gossans Gossans develop as iron sulfides decompose during surface and near-surface oxidation to yield sulfuric acid and soluble ferrous sulfate in reactions such as

$$FeS_2 + 3½O_2 + H_2O = FeSO_4 + H_2SO_4$$

The acid dissolves base-metal sulfides, and the ferrous sulfate oxidizes to leave mixed iron oxides. The end result is a porous network of filimentous, layered to concentrically developed iron oxides. A detailed discussion of the interpretation of gossans was prepared by Blanchard (1968), and a discussion of the nature and origin of gossans has been presented by Blain and Andrew (1977).

10.3 OPAQUE MINERALS IN COAL

Mineralogy

Major	Pyrite, marcasite
Rare	Arsenopyrite, chalcopyrite, bornite, sphalerite, galena, millerite, linnaeite, rutile, pyrrhotite, native sulfur
Associated Minerals	Quartz, calcite, dolomite, siderite, kaolinite, illite, gypsum, and a variety of secondary iron sulfates and iron oxides

Mode of Occurrence The sulfides are generally present in coal as (1) veins that are thin or film-like on the vertical joints (cleats), (2) lenses that range from millimeters to tens of centimeters across, (3) nodules or balls in which sulfides are intergrown with variable amounts of carbonates and clays, and (4) disseminated crystals and globules replacing organic matter.

Examples Virtually all known coal deposits contain sulfides, although the amount present is highly variable. Work in several coalfields has demonstrated a correlation of sulfide occurrence with the proximity of overlying marine strata, suggesting that sulfur may have been derived by bacterial reduction of seawater sulfate.

10.3.1 Mineral Associations and Textures

Sulfide minerals are the most well-known contaminants in coals, because they are major contributors to the total sulfur content of the coal and because they are often macroscopically visible. There is a strong tendency in the coal industry to refer to all sulfides generally as pyrite, and, although it is the dominant sulfide mineral, it is often not the only one present. Marcasite, the dimorph of

pyrite, is often present and intergrown with pyrite; minor amounts of sphalerite, galena, arsenopyrite, chalcopyrite, bornite, millerite, and linnaeite have been reported locally. Pyrite in the typical veins, lenses, and nodules is generally fine-grained and anhedral, as shown in Figure 10.5a. Individual layers within the lenses and nodules are usually composed of roughly equant, generally fine, anhedral grains. In some occurrences on cleats, especially where the sulfide is thin and disseminated, pyrite is intergrown with marcasite and exhibits a poorly developed radial growth structure. Marcasite appears to have been the primary phase in many occurrences and to have been subsequently converted in part to pyrite. Disseminated pyrite may be present either along cleats or within the residual structure of the organic matter. In the latter case, the pyrite frequently occurs as framboids, tiny spherical aggregates of pyrite euhedra, as shown in Figure 10.5b. Sphalerite has been extensively studied in the coals of Illinois (United States), where it occurs as cleat fillings (Hatch, Gluskoter, and Lindahl, 1976). The sphalerite contains up to 2.5 wt % Fe and as much as 1.3 wt % Cd. Its color is anomalous and includes gray-white and purple varieties; the cause of the coloration is not known.

10.3.2 Origin of the Opaque Minerals in Coals

The sulfides in coal constitute approximately one-half of the total sulfur content of the coal and are believed to have formed, for the most part, through the activity of sulfate-reducing bacteria during diagenesis. Studies of sulfur isotopes support this mode of origin of sulfur (Price and Shieh, 1979). The original sulfur content of the plant matter remains trapped in the organic substances now constituting the coal and was clearly insufficient to account for the bulk of the sulfide present in many coals. Although some disseminated pyrite, especially that occurring as frambroids, may have formed at the time of burial, most of the sulfide apparently formed during later diagenesis or metamorphism.

10.3.3 Coal Petrography

Coal is an organic rock composed of the organic equivalents of minerals called *macerals*. Macerals, the basic units of the Stopes-Heerlen system of coal petrographic nomenclature, are microscopically recognizable and distinctive organic constituents of coal. Instead of being defined by exact chemistries and relatively consistent crystallographic and reflectance properties as are minerals, the macerals are defined on the basis of the original plant components from which they were derived. Since deposition, the constituents have undergone gelification, carbonization (fusinization), and/or compaction, and/or fragmentation in the coalification process.

The macerals are not crystalline and vary widely in chemical composition and physical properties in response to variable degrees of compaction and heating. As used today, the term "maceral" describes both the shape and the

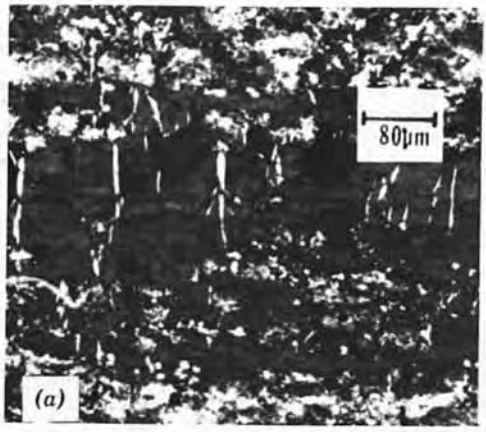

FIGURE 10.5 Opaque minerals in coal. (*a*) Anhedral grains of pyrite and pyrite-infilling cleats, Minnehaha Mine, Illinois. (Reproduced from F. T. Price and Y. N. Shieh, *Econ. Geol.* **74**, 1448, 1979, with permission of the authors and the publisher). (*b*) Typical framboidal pyrite in an Appalachian coal (width of field = 25 μm). (Photograph courtesy of Dr. F. Caruccio.)

nature of the microscopically recognizable constituents. The macerals are most easily distinguished in low-ranking coal; with increase in rank, the differences in reflectance diminish, because there is a general conveyance in chemistry and in physical properties (Figure 10.6).

Several types of macerals fluoresce green, yellow, or brown when irradiated

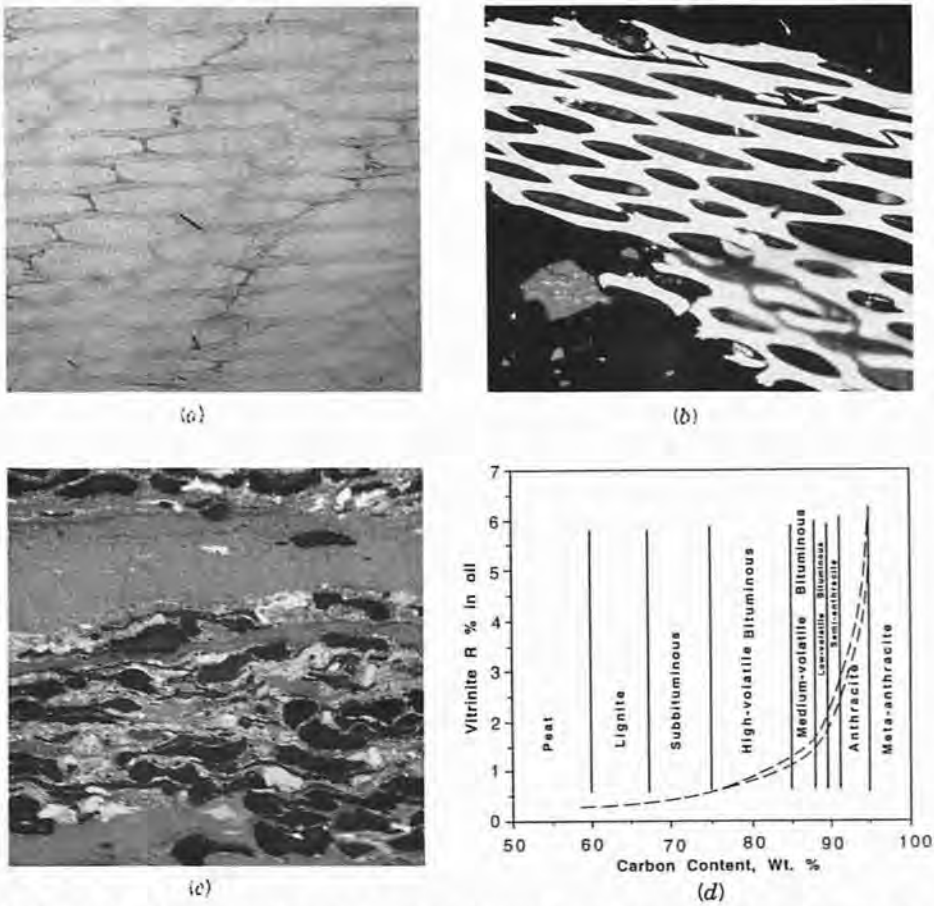

FIGURE 10.6 Coal macerals in Elkhorn No. 3 seam, high-volatile bituminous coal in Eastern Kentucky. (*a*) Vitrinite showing well-developed cell structure. (*b*) Vitrinite (gray) carring dark sporinite bodies and minor inertinite (white). (*c*) Fusinite particle showing typical xylem (wood) cell structure. (*d*) The reflectance of vitrinite, although a complex function as explained in the text, varies as a function of coal rank (each field of view is 200 μm oil immersion). (Photos courtesy of John Crelling.)

by blue or ultraviolet light. The color and intensity of the fluorescence depends on both the type of maceral and the rank of the coal. Fluorescence is greatest in the low-ranking lignites and sub-bituminous coals but is absent in high-ranking bituminous and anthracite coals. Detailed discussions of coal fluorescence are presented in Bustin et al. (1983) (where color plates also illustrate the fluorescence) and in the *International Handbook of Coal Petrography* (1975).

It has now been well established that the reflectance of vitrinite measured using oil immersion is a very reliable indicator of the rank of bituminous coals that have less than 30% volatile matter and of anthracites (Figure 10.6d). Hence, vitrinite reflectance measurement has become a standard analytical

technique in the examination of coals. Because the reflectance values are so low (less than 2% for most bituminous coals) relative to most ore minerals, it is necessary to have special low-reflectance glass standards. The actual relationships of reflectance, moisture content, hydrogen content, and carbon content are quite complex, and the reader is referred to Bustin et al. (1983) for greater detail.

All macerals may be classified in one of three major groups: (1) vitrinite, (2) exinite or liptinite, (3) inertinite. Unfortunately, the terminology in coal petrography is complex and sometimes confusing. For more detailed discussions, the reader is directed to the references given below.

Vitrinite—The most abundant macerals in bituminous coals, derived from woody tissue and bark; generally of moderate reflectance. The term *huminite* applies when used in describing lignite and sub-bituminous coal.
- Telinite—cell walls
- Collinite—structureless constituent of vitrinite
- Vitrodetrinite—fragmental or detrital vitrinite

Exinite or (liptinite)—Dark gray with low reflectance
- Sporinite—skins of spores and pollens (10^6/gm)
- Cutinite—outer layers of leaves or needles
- Resinite—natural resins usually occurring as round to elliptical droplets
- Alginite—algal remains, relatively dark
- Liptodetrinite—detrital fragments, similar to clays

Inertinite—Light gray to white, high reflectance
- Fusinite—cellular to "bogen" structure, with highest reflectance in bituminous coal; white to yellowish light in reflected light; high-polishing hardness
- Macrinite—amorphous nongranular ground mass of high R%
- Sclerotinite—fungal remains

10.4 URANIUM-VANADIUM-COPPER ORES ASSOCIATED WITH SANDSTONES AND UNCONFORMITY-TYPE URANIUM DEPOSITS

Mineralogy Different deposits show varying relative concentrations of minerals of the three metals, often with only one or two of the metals being present or greatly dominant. *Major minerals* from each metal are

Uranium	Uraninite (or its cryptocrystalline equivalent, pitchblende), coffinite [$U(SiO_4)_{1-x}(OH)_{4x}$], various types of asphaltic organic-matter-bearing uranium
Vanadium	Roscoelite (vanadium mica), montroseite [VO(OH)], and vanadium-bearing mixed-layer clay minerals

Copper	Chalcocite (ore related minerals of ~Cu_2S composition), bornite, chalcopyrite, covellite, native copper

Other (usually minor) minerals include a very large number of sulfides, notably pyrite, galena, sphalerite, gersdorffite, molybdenite, native gold and silver; silver sulfides. Secondary minerals include a very wide range of oxides, hydrated oxides, sulfates, and carbonates produced from the primary assemblages.

Mode of Occurrence Within conglomerates, sandstones and siltstones (particularly the reduced zones within red beds) as irregular masses of ore occurring as fillings of pore spaces, veinlets, and replacing organic materials, particularly fossil plants. Also as veins and veinlets closely associated with a major unconformity recording a period of continental weathering.

Examples The Colorado Plateau area of Colorado, Arizona, Utah, and New Mexico; Wyoming; Texas; the Athabasca Sandstone, Northern Saskatchewan; Darwin Area, Australia (the most important uranium-bearing examples). Copper-rich examples are very widespread—Corocoro, Bolivia; Udokan, Siberia. Many examples of limited or no economic importance are also known (e.g., Pennsylvania, United States; Alderley Edge, Cheshire, England).

10.4.1 Mineral Associations and Textures

The deposits of this group commonly occur in continental and marginal-marine clastic sediments that are considered as having been deposited under fluviatile-deltaic conditions. The bulk of these sediments have the distinctive red color due to fine-grained hematite and ferric oxyhydroxides, which lead to the term *red beds.* However, in contrast to the surrounding red sediments, the mineralized zones are often gray-greenish, containing a predominance of ferrous iron with relatively high sulfur and carbon concentrations. The mineralization occurs as lenses, pods, layers, or concave "rolls" that are grossly conformable with enclosing sediments, although cross cutting in detail. Most concentrations of mineralization are associated with organic debris, and some significant uranium deposits have resulted from the replacement of fossil logs.

The amounts of uranium, vanadium, and copper mineralization vary enormously both within and between deposits. The copper ores may also contain significant concentrations of silver. The ore minerals occur as veinlets and pore-space fillings in the sediments and as replacements of fossil plant matter. Often the cell structure of wood may be preserved, although totally replaced by uranium minerals and copper and iron sulfides (Figure 10.7). Although the major copper sulfide described from these deposits is "chalcocite," more recent descriptions of the complex phase relations in the Cu-S system (and the system Cu-Fe-S) suggest that much may remain to be learned regarding the

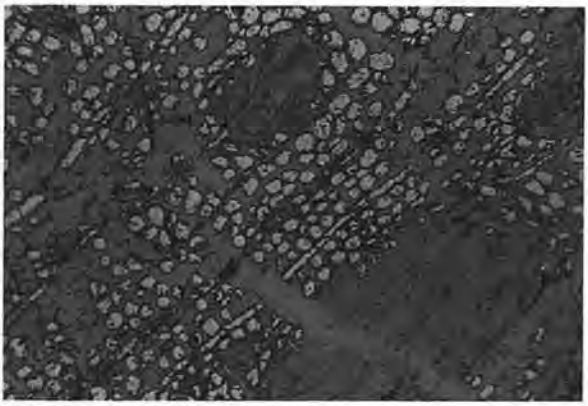

FIGURE 10.7 Pyrite replacing cellular structure in wood with associated chalcocite, Marysvale, Utah (width of field = 520 μm).

detailed mineralogy of these ores and the roles played by such phases as digenite, djurleite, and anilite (see Figure 10.8). A sulfur-rich bornite is common in many red bed deposits, where it may occur interstitially between sand grains or where it may selectively replace organic structures. The stability and mode of formation of this type of bornite remains an unresolved problem in phase relations of the Cu-Fe-S system. Pyrite is common in the reduced portions of the ores but is largely replaced by secondary hematite and hydrated iron-oxides in more oxidized areas.

At the Rabbit Lake, Cigar Lake, and Similas deposits, Northern Saskatchewan, mineralization is spatially related to the unconformity that underlies the Athabasca Formation, a fluviatile sedimentary sequence that includes red sediments with reduced zones and also carbonaceous materials. The mineralization has been studied in detail (Hoeve and Sibbald in Kimberley, 1978), and several stages, associated with oscillating episodes of oxidation and reduction, have been recognized. The earliest mineralization occurs as fracture or breccia infillings, with pitchblende as colloform encrustations and later massive mineralization associated with coffinite and sulfides. A second stage consists of veins of complex paragenesis, including euhedral quartz, carbonates, pitchblende, coffinite, sulfides, arsenides, and native copper. The final stage involves impregnation by sooty pitchblende and coffinite along fractures and joints and appears to be a reworking of pre-existing mineralization. Marmont (1987) presents a model of the origin of these deposits.

10.4.2 Origin of the Ores and Textures

It is widely accepted from overwhelming evidence that the ore minerals of this group were introduced later than the deposition of the host sediments. These ores are the result of precipitation from solutions passing through the sediments. The problems of origin concern the nature and source of the solutions,

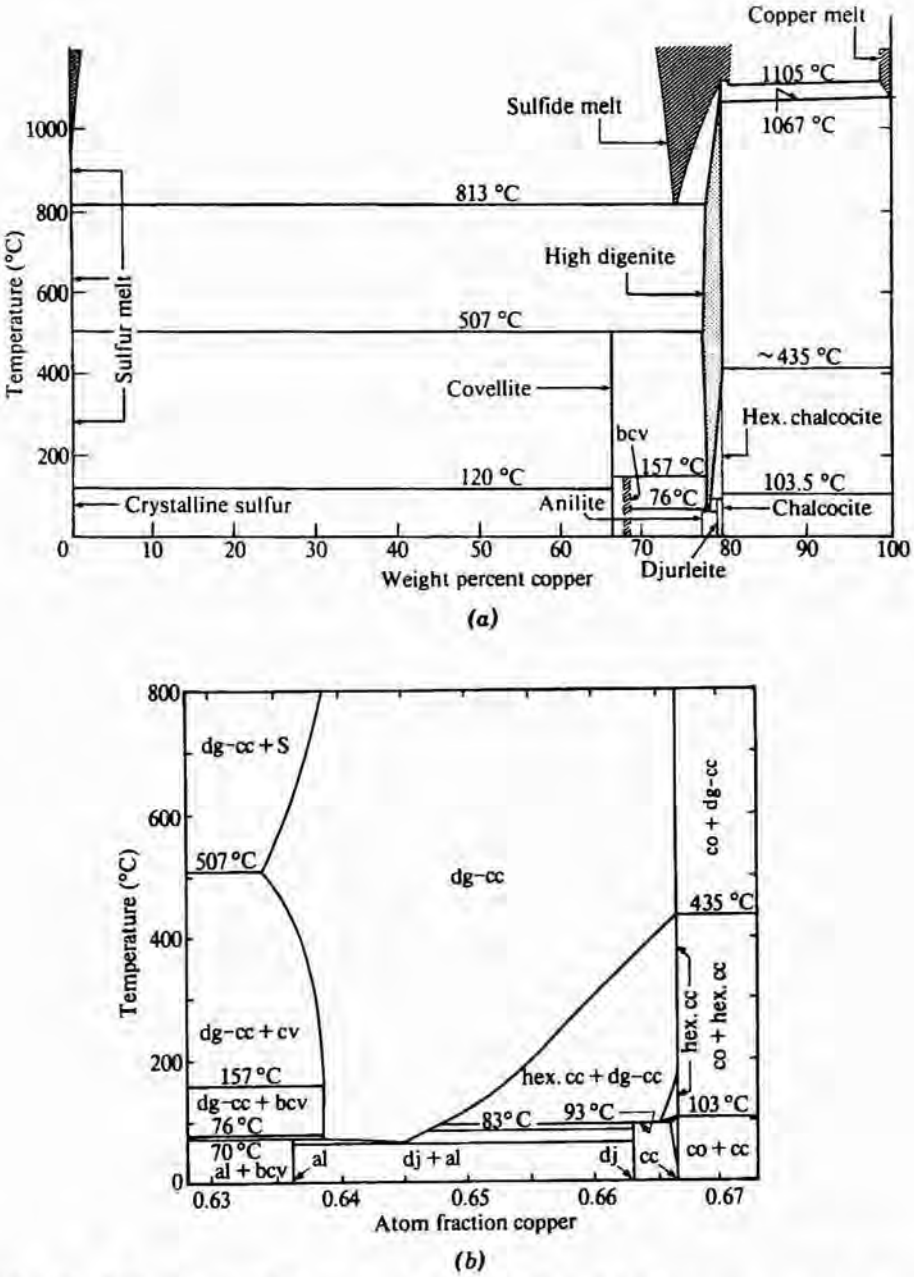

FIGURE 10.8 Phase relations in the system Cu-S. (*a*) Temperature-composition diagram of condensed phases. (*b*) Temperature-composition diagram of condensed phases in central portion of the system. Abbreviations: dg-cc, digenite-chalcocite; cv, covellite; al, anilite; dj, djurleite; co, copper. (From Vaughan and Craig, 1978.)

and their mode of transport and of precipitation. Three main suggestions have been made for the origin of the solutions.

It is widely accepted that the solutions were groundwater that leached metal ions and SO_4^{2-} ions from associated strata at low temperature and that the ore minerals were precipitated on encountering local reducing environments. The field relations of the major uranium-bearing deposits allow for large-scale leaching of underlying granites and other arkosic rocks and interspersed volcanic ash, which could supply the necessary metals. In oxidizing solutions, uranium can be transported as the relatively soluble uranyl $(U^{6+}O_2)^{2+}$ ion or as a carbonate complex such as $UO_2(CO_3)_3^{4-}$ or $UO_2(CO_3)_3^{-2}$. The relatively insoluble uranous (U^{4+}) ion is stabilized under reducing conditions, where it may precipitate out to form uraninite (UO_2), as shown in Figure 10.9. Since the mineralized zones are commonly gray-greenish (Fe^{2+}-rich) reduced areas, the concept of precipitation on encountering such areas appears sound. The formation of such localized reducing areas is commonly linked with the presence of organic matter. Bacterial activity in these areas could cause reduction of sulfate in the pore waters, which could react with introduced copper in solution to precipitate the highly insoluble copper sulfides. Vanadium could be transported as the V^{4+} ion and precipitated by reduction in the mineralized zone. The theory that organic reduction is important in the formation of the sulfide ores of this association is supported by data from sulfur isotopes. Fluid movement through porous sandstones often results in development of a "roll-type" deposit in which solution of U-V minerals occurs along an oxidizing surface that follows behind a reducing front where precipitation is occurring (Figure 10.10).

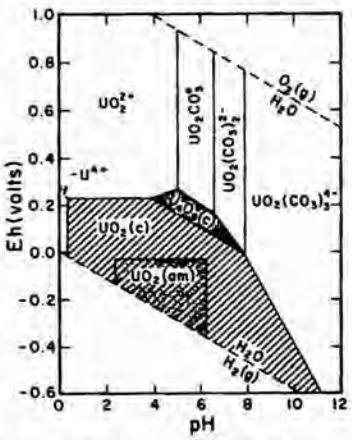

FIGURE 10.9 Eh-pH diagram in the U-O_2-CO_2-H_2O system at 20°C for $P_{CO2} = 10^{-2}$ atm, showing the stability fields of amorphous UO_2[UO_2(am)], ideal uraninite [UO_2(c)], and U_4O_9(c). Solid solution boundaries are drawn at 10^{-6}M (0.24 ppm) dissolved uranium species. (After D. Langmuir in Kimberley, 1978; used with permission of the author.)

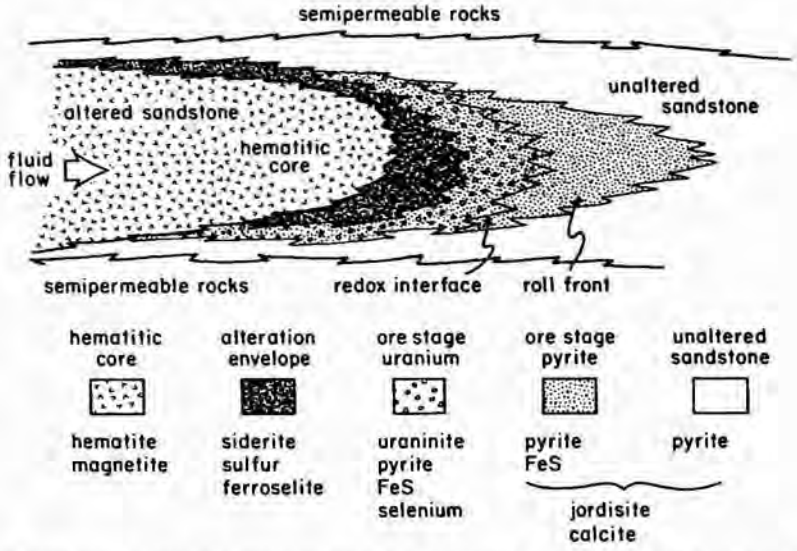

FIGURE 10.10 Idealized cross section of a "roll-type" uranium deposit. (After Granger and Warren, 1974.)

An alternative suggestion for the origin of the mineralizing solutions is that they were derived directly from igneous rocks at depth (i.e., of igneous/hydrothermal origin). Such solutions would have to pass up through fractures into the sedimentary hosts in which precipitation could occur through the same processes already outlined. The general absence of large feeder veins, the

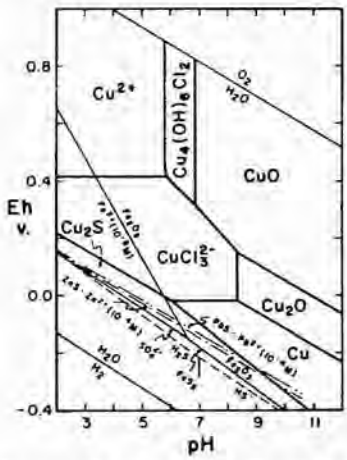

FIGURE 10.11 Eh-pH diagram for the sysem Cu-O-H-S-Cl at 25°C ($\Sigma S = 10^{-4}$ M, $Cl^- = 0.5$ M as NaCl, boundaries of Cu species at 10 M). Boundaries are also shown for some Fe- and S-bearing species; the stability of copper sulfides other than chalcocite is not shown. (After A. W. Rose, *Econ. Geol.* **71**, 1041, 1976; used with permission.)

vast lateral extent of such examples as the great Colorado Plateau deposits, and the absence of a universal association with igneous sources are major arguments against this theory. A third view combines the first two theories by deriving the solutions from mixing of hydrothermal and meteoric solutions.

Work by Rose (1976) on the copper deposits of this association has drawn attention to their geological association with evaporites, which could have furnished chloride-rich groundwaters. In most normal oxidizing groundwaters, the solubility of copper is less than 1 ppm at reasonable pH values. However, in chloride-containing solutions, the cuprous ion forms the complexes $CuCl_2^-$ and $CuCl_3^{2-}$, which allow solubilities of ~100 ppm copper in 0.5 m Cl^- at pH 7.0 and intermediate Eh. As illustrated in Figure 10.10, the $CuCl_3^{3-}$ complex is stable underl pH/Eh conditions compatible with the presence of hematite. The solutions transporting copper are believed to be in equilibrium with hematite, quartz, feldspar, and mica, and at temperatures below ~75°C. The general relationships illustrated in Figure 10.11 (at 25°C) therefore apply, so that reduction will bring about precipitation of copper as copper sulfides.

10.5 MODERN PLACER DEPOSITS

Mineralogy Placer mineral deposits, having been formed as the result of the mechanical accumulation of grains from pre-existing deposits, can contain a wide range of minerals. The discussion below treats the most common and important types of placer deposits.

Major minerals	Ilmenite, rutile, magnetite, cassiterite, gold (commonly called electrum if silver content exceeds 20 wt %)
Minor minerals	Platinum group minerals, hematite

Mode of Occurrence Modern placer deposits typically occur as sandbars or bottom sands in rivers and streams or in the bank materials that are deposited during episodes of high water flow. They also occur in modern coastal beaches as thin, irregular, and discontinuous layers and lenses of dark minerals. Unconsolidated paleoplacers at least as old as Tertiary in age are found on river terraces and as blankets of sands and gravels adjacent to rivers and streams that have become more deeply incised or that have migrated laterally. Paleo-beach placers occur in continental shelf sediments where sea level has risen relative to the land surface or in beach terrace deposits where sea level has fallen relative to the land surface. Examples are Eneabba, Yoganup, Western Australia; North Stradbroke Island, Queensland, Australia; Trail Ridge and Green Cove Springs, Florida.

10.5.1 Mineral Associations and Textures

Placer deposits generally consist of accumulations of individual grains that have survived weathering and that have been fortuitously brought together

because of size (usually 1 mm and smaller) and specific gravity. Accordingly, original mineral associations are generally not preserved. In contrast, many grains preserve at least some of their original internal textures. The **ilmenites**, which constitute the most abundant ore mineral in most placer occurrences, and the "black sands" in most streams, vary from homogeneous single crystals to complex lamellar intergrowths with hematite (Figure 10.12). Exposure of the grains to marine, fluvial, or interstitial ground water causes leaching of the ilmenites, resulting in slow removal of the iron with a consequent increase in the titanium content of the remaining, somewhat porous material. The leaching dissolves hematite more rapidly than ilmenite; hence, it is common to find grains in which either the outer lamellae of hematite or all of the hematite have been dissolved away, leaving only oriented lamellae-like holes (Fig. 7.32).

Magnetite may be locally abundant in placer deposits, but it tends to oxidize rapidly. Hence, magnetite grains are frequently oxidized to hematite or goethite around margins and along cleavage planes (see Fig. 7.34). **Rutile** is less abundant than ilmenite but is more resistant to oxidation and solution. Hence, it usually occurs as reddish equant grains, occasionally with inclusions of ilmenite.

Cassiterite is also very resistant to oxidation and solution effects, and thus shows little change in the placer environment other than surficial abrasion, which reduces grain size and makes grains more spherical. Reflected-light examination of cassiterite generally reveals only an apparently homogeneous phase, with occasional inclusions of silicates or other oxides. Breccia-like textures in the grains suggest periods of deformation during formation, probably long before liberation as a placer grain. Examination of doubly polished thin sections of placer cassiterite may, however, reveal well-developed growth zoning and have oriented lamellar to needle-like inclusions of ilmenites (Figure

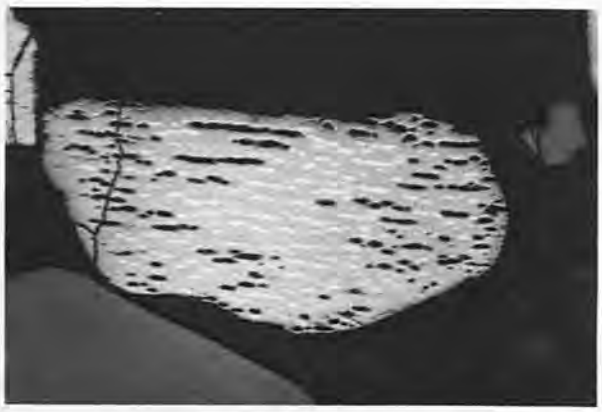

FIGURE 10.12 Placer ilmenite with lenses of hematite (white) that have been dissolved out, especially around the edges. The removal of the hematite increases the titanium content of the grain. Lilesville, North Carolina (width of field = 600 μm).

FIGURE 10.13 Oriented lamellae of ilmenite within a placer grain of cassiterite, Shelby, North Carolina (width of field = 600 μm).

10.13), and zones or clouds of fluid inclusions. Cassiterites may also contain inclusions of tantalum and niobium phases like tapiolite and columbite.

Placer **gold** grains were long considered chemically inert and hence only modified by physical abrasion during transport in the placer environment. Although many gold grains are homogeneous when examined in reflected light, many others display inclusions of minerals that coexisted in the original lode occurrence (e.g., tellurides) or that were incorporated mechanically during transport (e.g., iron hydroxides, quartz). Several recent studies have also demonstrated that placer gold grains commonly display the presence of sharply bounded, irregular to continuous rims of high-purity gold (>950 fineness or 95 wt % Au) around their margins. These high-purity zones (Figures 10.14 and 7.33) may also appear internally, where they are developed along fractures or within cavities in the gold grains. These gold-rich zones are clearly visible because of the color difference in reasonably polished grains, but they may be enhanced by etching using 2% NaCN or KCN (use with great caution and **NEVER** allow the solution to become acidic) and the use of oil immersion.

10.5.2 Origin of the Ores

Placer ores form when resistant original (primary) mineral grains are weathered out, transported (usually by rivers), and mechanically concentrated. Ilmenite and rutile occur as accessory phases in a wide variety of igneous and metamorphic rocks from which they are liberated during decomposition. Accumulations of these minerals are very common in rivers and streams and, locally, in beaches, where they constitute the "black sands"; such accumulations are nearly always too small in volume to be of economic value. Large mineable deposits, such as Eneabba and Green Cove Springs, are believed to have formed through the winnowing out of the lighter quartz grains by intense

FIGURE 10.14 Placer electrum grain (approximately 80 wt % gold) on the lower side of which a high-purity (greater than 95 wt % gold) rim has developed. The boundary between the core of the grain and the rim is very sharp, Lilesville, North Carolina (width of field = 600 μm).

storm-driven wave action and the accumulation of the heavier ilmenite and rutile (and associated heavy minerals such as garnet, zircon, etc.) along beach ridges or headlands.

Placer gold and cassiterite may occur in beach-type deposits similar to those that contain major titanium sand deposits. More commonly, however, placer gold and cassiterite occur in river beds and adjacent sediments where these minerals have settled after periods of episodic movement. Most transport occurs during flood periods when the higher velocities can scour and dislodge grains from their previous sites. Obstructions, changes in channel shapes, or decrease in water flow results in the selective sorting of minerals according to size, shape, and specific gravity. This may allow sufficient concentration of gold or cassiterite to form economically significant deposits.

10.6 GOLD-URANIUM ORES IN ANCIENT CONGLOMERATES

Mineralogy Major pyrite; gold (as native metal with some silver) may be a major ore mineral; uranium in uraninite, "thucholite" (a uraniferous hydrocarbon), or brannerite (a complex uranium-bearing silicate) may also be of major importance. Osmiridium (OsIr) may be of minor economic importance.

Associated sulfides of no economic significance may include marcasite, pyrrhotite, sphalerite, galena, molybdenite; also arsenides and sulfarsenides containing Co and Ni may occur.

Detrital heavy minerals may include chromite and zircon, ilmenite, magnetite, rutile, and various mafic silicates. The remainder of the ore material is

largely made up of quartz, with significant feldspar, sericite, chlorite, and chloritoid.

Mode of Occurrence The gold and uranium ores occur disseminated in beds and lenses of coarse conglomerate which are parts of arenacecus sequences. Generally, the conglomerates are of quartz pebbles and appear to be of fluviatile or shallow-water deltaic origin. The major examples are Precambrian in age.

Examples Two very important examples are the Witwatersrand, South Africa (major gold and uranium deposit) and Elliot Lake (Blind River), Ontario, Canada (major uranium deposit); Jacobina, Brazil, is a less important gold deposit.

10.6.1 Mineral Associations and Textures

The ore minerals of gold and uranium are generally very fine-grained (commonly not visible except under the microscope). They commonly occur interstitially to the conglomeratic fragments, with gold as grains and pore space fillings, although they occur occasionally as fine veinlets. Uraninite, thucholite, and brannerite occur as detrital grains and in some cases as colloform sheets or as veinlets, and gold and uranium show a strong tendency to occur together. Osmiridium in the Witwatersrand ores is partly intergrown with gold. Pyrite, found in concentrations of 2–12% by volume in the conglomerates has been described by Ramdohr (1958) as being of three textural types:

1. *Allogenic.* Having rounded outlines and a smooth homogeneous interior.
2. *Concretionary authigenic.* Having a structure composed of loosely aggregated fragments.
3. *Reconstituted authigenic.* Loosely aggregated fragments that have been partially recrystallized.

A detailed account of the mineralogy of Witwatersrand ores is given by Feather and Koen (1975). Examples of both the textural varieties of pyrite and the occurrence of gold in the Witwatersrand ores are shown in Figures 10.15a, and 10.15b. A typical colloform texture of the uraninite is shown in Figure 10.15c. Ore concentrations are usually greatest where the conglomerates are thickest, and, in the Witwatersrand ores, the silver content of the gold (which ranges from ~5 to 16 wt %) shows systematic variation, decreasing with depth in any single ore lens ("reef"). High gold concentrations also occur in very thin carbonaceous seams, and much of the gold in the conglomerates may represent the reworking of such material.

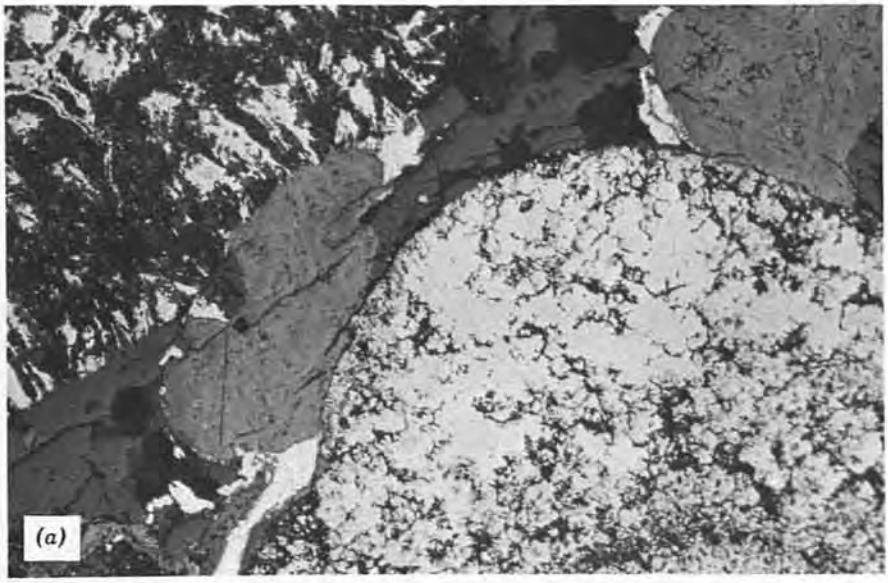

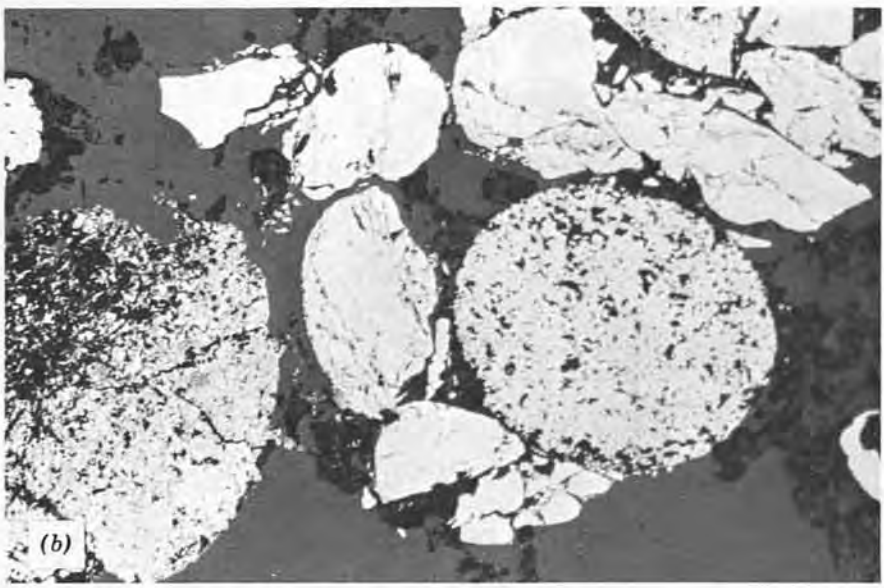

FIGURE 10.15 (*a*) Native gold (light gray) occurring around the margins of quartz grains and pyrite aggregates, Witwatersrand, South Africa (width of field = 2,000 μm). (*b*) Pyrite of allogenic and concretionary authigenic textural types, Witwatersrand, South Africa (width of field = 2,000 μm). (*c*) Colloform uraninite with associated fine pyrite (width of field = 2,000 μm).

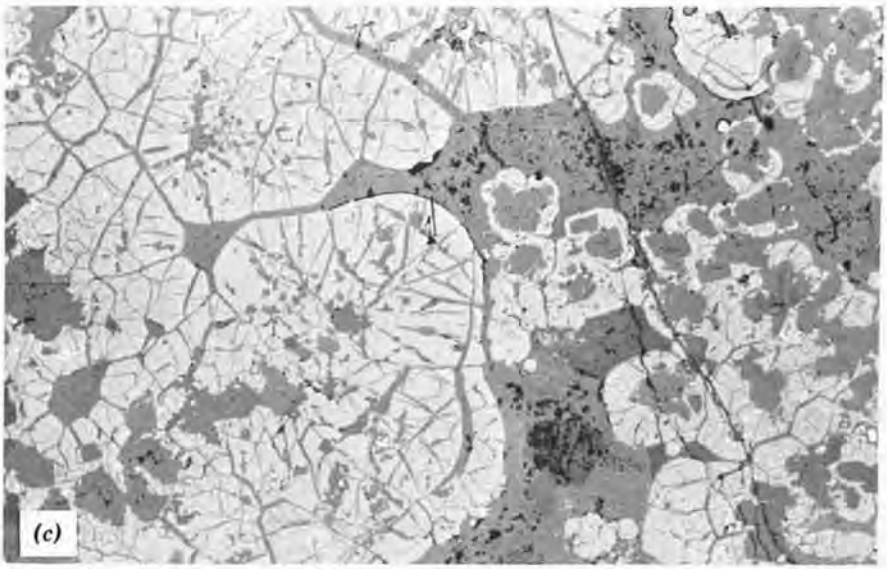

FIGURE 10.15 *(Continued)*

10.6.2 Origin of the Ores

Historically, three main theories have developed regarding the origin of these ores.

1. *Placer theory.* The ore minerals have been derived by erosion of adjacent areas, have been transported, and have been deposited by streams along with the comglomerates. Even among the proponents of the placer theory, there are significant differences regarding the location of the original sources of the gold-bearing rocks and the distances of transport (Minter, 1978, 1990, 1991; Minter et al, 1993; Hutchinson and Viljoen, 1986).
2. *Hydrothermal theory.* The gold, uranium, and some of the other metals have been introduced in hot aqueous solutions derived from an external source, such as an igneous intrusion. Phillips (1989) has argued that gold is primarily epigenetic, having been introduced by hydrothermal fluids that entered the sediments during metamorphism. The close connection between the gold and the sedimentary facies is explained as resulting from the ore fluids reacting with pyrite and organic matter in selected environments.
3. *Modified placer theory.* The ore minerals, having been deposited as placers, have been locally redistributed within a particular orebody. There is ample evidence that gold-bearing beds have been subjected to greenschist facies metamorphism and that there have been aqueous fluids circulating through the rocks (Frimmel et al., 1993).

The occurrence of gold and of uranium mineral veinlets suggest at least some textural modification, so the major disagreement on origin has been between a modified placer theory and a hydrothermal theory. Most workers favor a modified placer origin for these deposits.

Specific arguments concerning the origin of the Elliot Lake and the Witwatersrand deposits are outlined by Derry (1960) and by Pretorious (1975, 1976).

10.7 LEAD-ZINC DEPOSITS IN CARBONATE ROCKS AND OTHER SEDIMENTS

Mineralogy

Major	Galena and sphalerite are the metalliferous ore minerals. Barite and fluorite are locally economically important. Pyrite and marcasite are widespread, and so is chalcopyrite, although it is rarely significant as a source of copper.
Minor	Sulfides that may occur in minor amounts include wurtzite, greenockite, millerite, bravoite, siegenite,bornite, covellite, enargite, luzonite. A variety of oxides (hematite, cuprite, limonite), carbonates (e.g., smithsonite, cerussite, malachite), and sulfates—for example anglesite, jarosite [$KFe_3(SO_4)_2(OH)_6$]—result largely from the alteration of the major sulfides.
Gangue Minerals	Dominantly calcite, dolomite, aragonite, fluorite, and quartz. Siderite, ankerite, gypsum, and colloform silica may also occur.

Mode of Occurrence The ores nearly always occur in sedimentary carbonate host rocks, particularly dolomites, but also in limestones and magnesian limestones. They may also be found in associated sandstones, shales, or conglomerates. Many of the larger orebodies occur as stratiform masses (i.e., parallel, or nearly so, with the bedding), but others occur as vein infillings (or sometimes replacements) along fissures (commonly faults or joints) that may cross the bedding. Often the carbonate host rock constitutes part of a reef (i.e., is biohermal), and the ores are localized relative to a particular reef facies. In other cases, the ores may occur in association with a solution collapse breccia related to karst and paleoaquifer development.

Examples The most important examples occur in Paleozoic and Mesozoic carbonate sediments, particularly in North America, Europe, Russia, and North Africa. Principal areas of early exploitation were in the Triassic sediments of the Eastern Alps (hence the label "alpine type") and in the upper and

middle regions of the Mississippi Valley of the United States (hence "Mississippi Valley type") within Paleozoic sediments. Within the latter area, the "Tri-State" field (around the Missouri-Kansas-Oklahoma border), an important early mining district, has been superseded by the Old and New (= Virburnum Trend) Lead belts of southeast Missouri. Other major North American occurrences are in the southern Appalachians, especially Tennessee, and the Pine Point area, Northwest Territories, Canada. The deposits of the English Pennines, although now little exploited, have been the subject of much scientific study. Other notable European examples occur in Central Ireland and in Silesia. Similar lead-zinc ores (e.g., Laisvall) occur in the Lower Cambrian and uppermost Precambrian sandstones along the western border of the Baltic Shield in Norway and Sweden.

10.7.1 Mineral Compositions, Textures, and Paragenesis

The simple mineral assemblages that are characteristic of these deposits are made up of a few well-crystallized phases of simple composition. The galena is characteristically lower in silver content than is the galena of many vein-type ores (see Section 9.6), and the sphalerite is commonly pale in color, with highly variable but generally small amounts of iron and manganese substituting for zinc. The sphalerite does commonly carry a relatively high cadmium content (in some cases, greenockite, CdS, being an accessory mineral) and may contain economically recoverable germanium (e.g., in Central Tennessee).

The textures exhibited by the ores in polished section and on a larger scale, although varying with the particular occurrence, are also relatively simple. In the larger orebodies, the phases occur as large, irregular polycrystalline aggregates within the host rock. When the sulfides occur in veins or as breccia fillings, they may be massive or may provide beautiful examples of crustification, with delicately developed symmetric or asymmetric bands occurring parallel to the margins of the veins (see Figure 8.4a). Alternating bands of very fine-grained sphalerite and wurtzite found in these ores are termed *schalenblende*. Colloform textures are also common in both vein ores and the *breccia ores* associated with solution collapse brecciation. These textures may involve the layered intergrowth of sphalerite and wurtzite, galena, pyrite, and marcasite, or other sulfides and nonsulfides. The free growth of crystals on the walls of solution cavities can also produce large, well-formed crystals (e.g. the Elmwood Mine in Central Tennessee frequently yields 20 cm fluorite cubes and 40 cm or larger calcite crystals). Much of the ore in these deposits consists, therefore, of crystals deposited one upon another in open space. Examples of characteristic textures are shown in Figures 10.16, 7.3a, and 7.3b.

The paragenetic sequences reported for these deposits can be illustrated through a number of examples. In Figure 10.17, a paragenetic diagram for the Tri-State deposits based on the work of Hagni and Grawe (in Hagni, 1976) is shown. Although the sequence is generalized and a number of aspects are controversial, it illustrates the characteristically repetitive nature of this style of

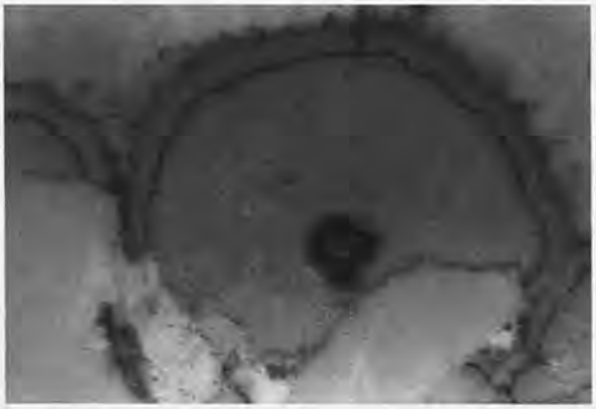

(a)

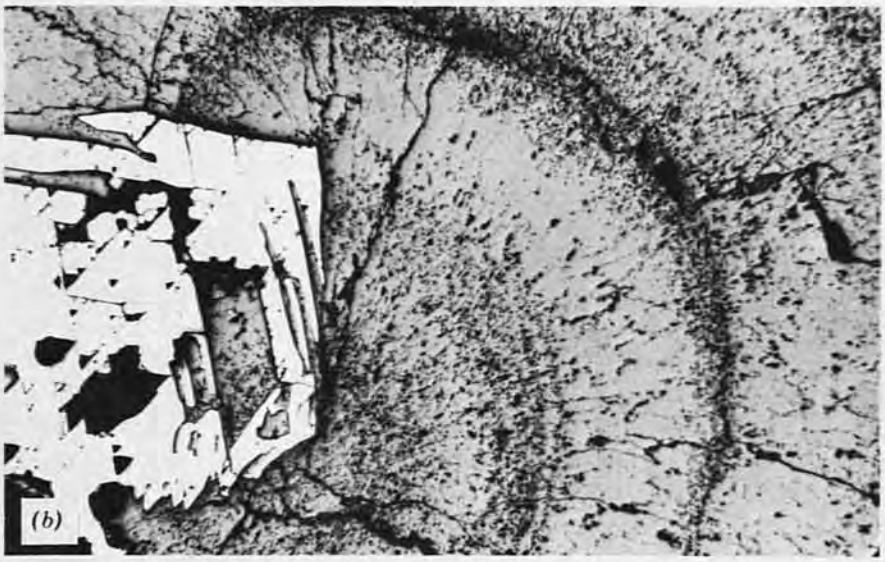

FIGURE 10.16 Characteristic textures of lead-zinc ores in carbonate rocks. (*a*) Concentric growth of sphalerite on dolomite fragments. The sphalerite contains a central core and a thin band made black by the presence of hydrocarbons; these zones are also abnormally enriched in cadmium and contain traces of lead and copper, Idol Mine, Tennessee (width of field = 1,200 μm). (*b*) Skeletal galena crystal (white) overgrown by concentric bands of sphalerite, Pine Point, Northwest Territories (width of field = 2,000 μm). (*c*) Early pyrite subhedra associated with a later veinlet of galena in a dolomite host, Austinville, Virginia (width of field = 2,000 μm).

mineralization (several periods of sphalerite deposition in this case). Another example is the Magmont Mine (southeast Missouri), where Hagni and Trancynger (1977) recognized three phases of mineralization—early disseminated mineralization, followed by colloform sulfides, followed by crystalline sulfides, quartz, and calcite in fractures and vugs. Overlap and repeated deposi-

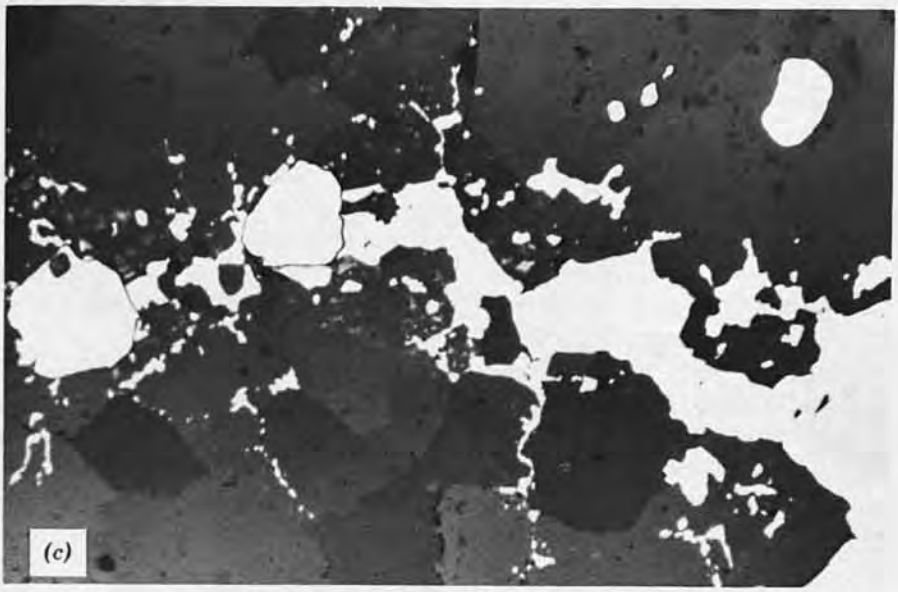

FIGURE 10.16 (*Continued*)

tion of sulfides occurred throughout the episodes of mineralization, with galena and chalcopyrite deposited during six intervals; deposition of sphalerite, marcasite, and pyrite occurred during four intervals; deposition of dolomite and quartz occurred during three intervals. In the South Pennine Orefield (England), the primary sulfide mineralogy is remarkably uniform and displays a consistent paragenetic sequence of bravoite, nickel-rich and

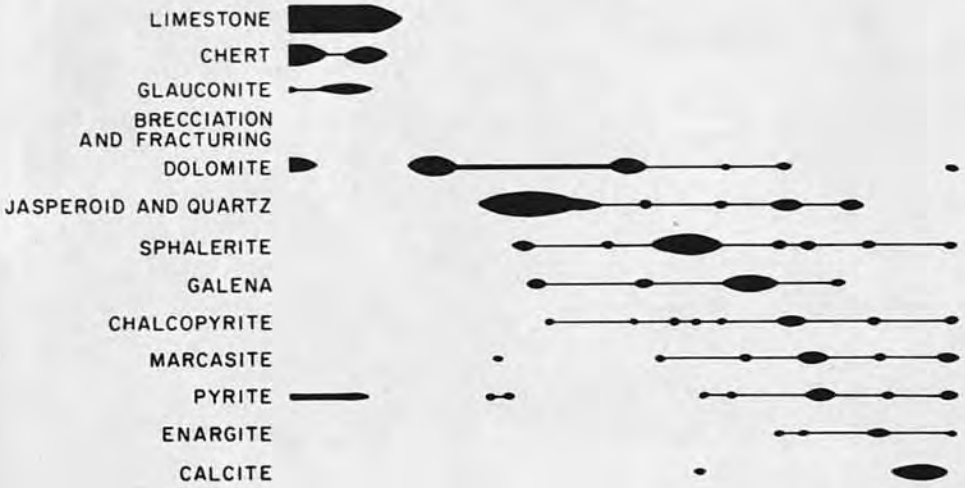

FIGURE 10.17 Paragenetic diagram for the Tri-State ore deposits (After R. D. Hagni and O. R. Grawe, *Econ. Geol.* **59**, 455, 1964; with the publisher's permission.)

nickel-poor pyrite and marcasite, chalcopyrite, galena, and sphalerite (Ixer and Townley, 1979) similar to that discussed and illustrated in detail in Section 8.3.3, whereas greater diversity is exhibited in the Northern Pennine Orefield (Vaughan and Ixer, 1980). The importance of nickel as a minor element in "Mississippi Valley-type" mineralization is also highlighted by these authors. Although the major mineral assemblages of these ore deposits are both simple and uniform, commonly there is evidence for a zonal distribution in terms of minor elements. The lead-zinc ores of several districts contain hydrocarbons in fluid inclusions, as bands in sphalerites, and even as droplets that occur on or between crystals. Consequently, hydrocarbons may play a part in the deposition of the ores (Anderson, 1991).

Along the western border of the Baltic Shield in Norway and Sweden, most notably at Laisvall in Sweden, lead-zinc mineralization is confined to sandstones. The assemblage includes pyrite, calcite, barite, flluorite, galena, and sphalerite filling the interstices of the sand grains (Figure 10.18). Although the host rock is different, these ores appear to be closely related to the lead-zinc ores of carbonate rocks (Bjørlykke and Sangster, 1981).

10.7.2 Ore Formation

The literature describing lead-zinc ore deposits in carbonate rocks and discussing their genesis is very considerable. Important literature descriptions

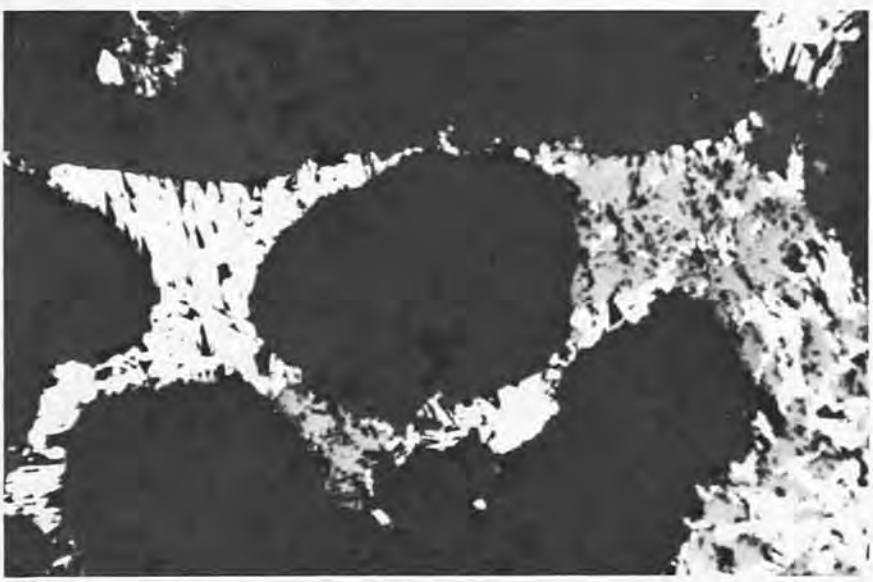

FIGURE 10.18 Galena (light gray) and sphalerite (medium gray) infilling around quartz grains, Laisvall, Sweden (width of field = 2,000 μm).

include the monograph edited by Brown (1967) and studies by Beales and Jackson (1966), Heyl (1969), Brown (1970), Anderson (1975, 1991), Sangster (1976), Anderson and MacQueen (1982), Sverjensky (1986), and Ixer and Vaughan (1993). Despite the considerable amount of work undertaken on these ores, their origin remains controversial.

The characteristically simple mineralogy and the localization of ore in carbonate host rocks (sometimes in particular facies, sometimes in specific tectonic or karstic structures) have already been emphasized. The vein-type ores clearly have resulted, in many cases, from successive deposition from introduced (predominantly aqueous) solutions. Fluid inclusion studies have indicated that these were saline solutions that deposited the minerals at temperatures below ~200°C, frequently below ~100°C, but the origin of these fluids remains controversial. As to the origin of the "stratiform" orebodies, theories ranging from syngenetic to wholly epigenetic have been propounded. In 1970, Brown stated that North American opinion favored a "dominantly connate marine but epigenetic ore fluid with probably minor additions from deeper sources" and that European opinion was "divided almost equally between proponents of syngenesis-diagenesis and of magmatic epigenetic origin."

Since 1970, particular emphasis has been placed on the problems of transport and deposition of the metal sulfides. Many have supported the view that connate brines have acted as a means of transporting metals (as chloride complexes) and that mixing with a separate H_2S-rich fluid in the limestone environment has caused sulfide precipitation (e.g., Beales and Jackson, 1966; Anderson, 1975). Hydrocarbons in the limestones and sulfate-reducing bacteria have been cited as important in the conversion of dissolved sulfate to sulfide and the spacial link of Mississippi Valley deposits to oilfield-like brine sources emphasized. The conflict between the European proponents of a syngenetic-diagenetic origin (largely those workers studying the Eastern Alps) and the proponents of an epigenetic origin has been somewhat clarified by Sangster (1976). He has proposed a division into two major classes of lead-zinc deposits in carbonates.

1. Mississippi Valley type, which are "stratabound" and were emplaced after lithification of the host rocks (i.e., epigenetically) into "open space" provided by a variety of structures (e.g., Mississippi Valley, Pine Point, English Pennines).
2. Alpine type, which are "stratiform" and also synsedimentary in large part. Here the original source of the ores is regarded as contemporaneous with the host rocks and is linked to submarine volcanism. Remobilization may have resulted in concentration of these ores and the formation of epigenetic features (e.g., the Eastern Alps, Central Ireland).

10.8 STRATIFORM BASE-METAL SULFIDE ORES IN SEDIMENTARY ROCKS

Mineralogy

Major	Pyrite; chalcopyrite or galena and sphalerite; in some ores, pyrrhotite, bornite, chalcocite (also digenite, djurleite), or even native copper may be major and cobalt sulfides (carrollite), or sulfarsenides may be economically important. Cobalt also substitutes in pyrite.
Minor	Arsenopyrite, tetrahedrite, native bismuth, bismuthinite, argentite, niccolite; molybdenite, covellite, and other sulfides may occur.
Gangue Minerals	Carbonates, barite, fluorite.

Mode of Occurrence These are disseminated to massive stratiform sulfide ores that are generally conformable within sedimentary sequences in which they occur and grade into the ores discussed in Section 10.9. The host rock may be a black shale, dolomite or, more rarely, an arenaceous unit (e.g., quartzite) and may be of considerable lateral extent. The host sediments may be undisturbed or may have undergone mild folding and metamorphism.

Examples Kupferschiefer-Marl Slate of Northern Europe; Copperbelt of Zambia and Zaire; White Pine, Michigan, United States; Selwyn Basin, Yukon, Canada; Mt. Isa, Broken Hill, Australia.

10.8.1 Mineral Associations and Textures

The ore minerals of this association are characteristically fine-grained and disseminated in the host rock often as lenses comformable with the bedding (Figure 10.19). A characteristic texture found in the sulfides, particularly pyrite, is the framboid (Figure 10.20). Also common are colloform textures in pyrite, galena, and sphalerite. Most of the sulfides occur as anhedral grains but pyrite is one of the few sulfides that may be euhedral. The ore minerals generally occur as random aggregates, although intimate intergrowth textures involving laths, intersecting spindles, or myrmekitic fabrics occur between the copper and copper-iron sulfides. The intergrowths of bornite and chalcopyrite are clearly a result of exsolution and other intergrowths involve bornite with chalcocite or other copper sulfides (Figure 10.21) (the precise identity of many of the copper sulfides in these ores has never been checked). Some of the more deformed ores of this type contain very minor development of mineralized veins.

An important characteristic of these ores is the presence of a zonal distribution of ore metals on a regional or a more local scale. In the White Pine deposit, for example, in passing stratigraphically upward through the host shales, a

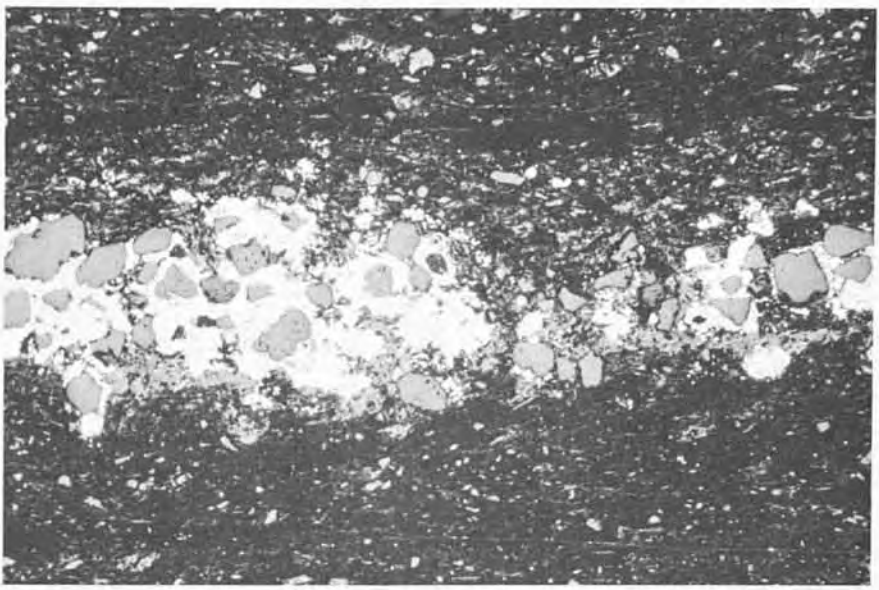

FIGURE 10.19 Fine-grained lens of pyrite with minor chalcopyrite; the lighter gray subhedra are of quartz, Marl Slate, Northern England (width of field = 300 μm).

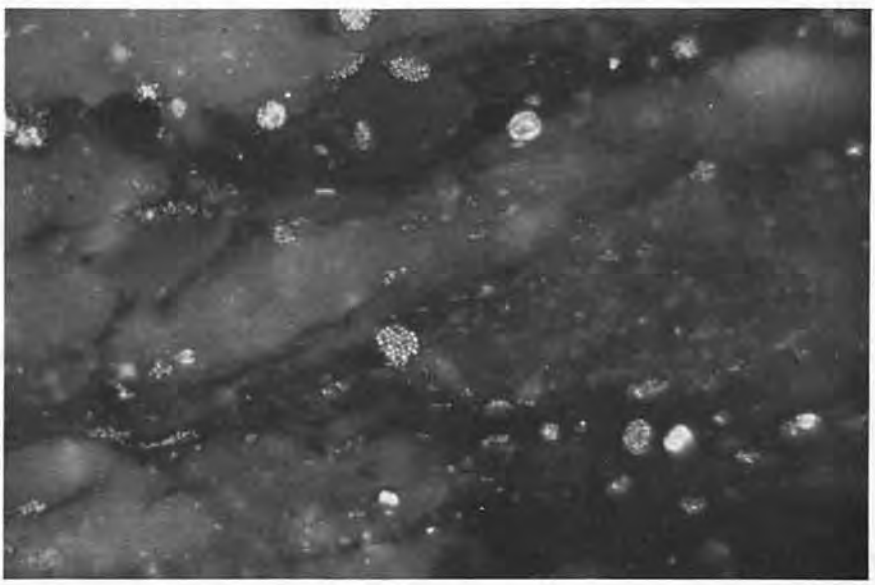

FIGURE 10.20 Finely dispersed pyrite framboids in dolomite, Marl Slate, Northern England (width of field = 300 μm).

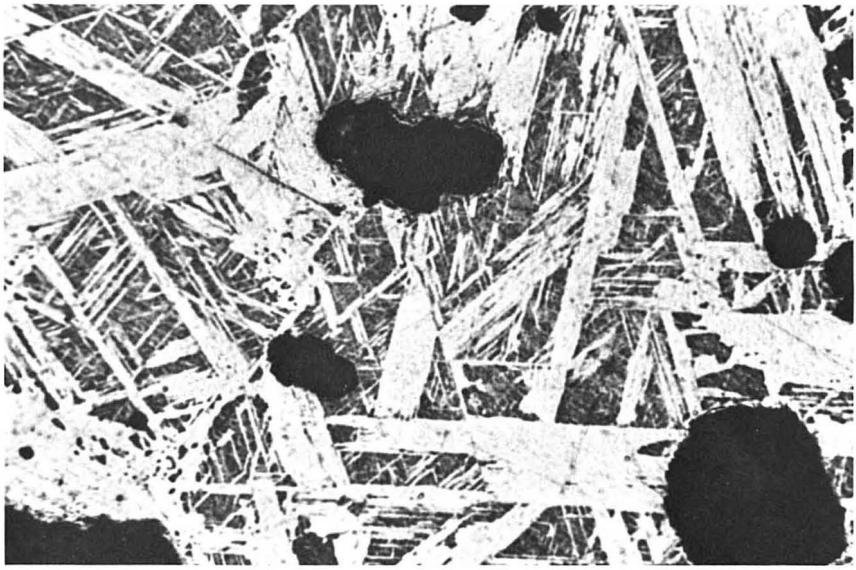

FIGURE 10.21 Intergrowth of bornite (dark gray) and chalcocite (light gray), which has formed as a result of exsolution of an originally homogeneous solid solution, Kolwezi, Katanga, Zaire (width of field = 300 μm).

sequence of copper, chalcocite, bornite, chalcopyrite, pyrite is observed (Brown, 1971). In certain Zambian deposits, a sequence bornite → chalcopyrite → pyrite has been related to syngenetic sulfide concentrations in shales deposited in progressively deeper water (Fleischer, Garlick, and Haldane, 1976).

Metamorphism of stratified synsedimentary ores often results in their recrystallization while preserving their intimate stratified nature. This is evidenced by the development of coarser equigranular annealed textures in the sulfides and the growth of micas (Figure 10.22). Intense metamorphism results in disruption of the finely laminated structure and the development of the textures described in Section 10.10.

10.8.2 Origin of the Ores

Ore deposits of this type are still among the most controversial with regard to their origin. The pronounced bedded character of the ores has led authors to propose that they are directly deposited sulfide-rich sediments (i.e., are syngenetic) and that euxinic conditions in the depositional basin were combined with an influx of metals from an erosional source to produce the ores and their zonal distribution. Problems of introducing sufficient metals have commonly led to suggestions of submarine volcanic springs as a source.

The opposing view regarding origins is that the ores were introduced by mineralizing solutions after formation of the sediments (i.e., the ores are epigenetic) and were selectively precipitated to replace and pseudomorph

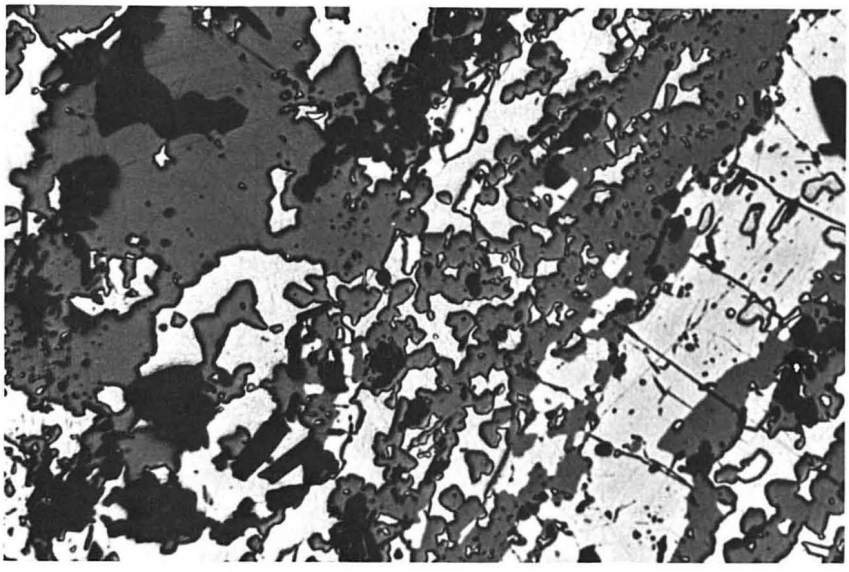

FIGURE 10.22 Primary depositional banding retained through metamorphism. Recrystallization of the ores, primarily galena, but with minor pyrrhotite and sphalerite in the band shown, has been accompanied by the growth of micas (dark laths), Sullivan Mine, British Columbia (width of field = 2,000 μm).

characteristically sedimentary structures. Commonly, the metals in this case have been regarded as derived through leaching of associated rocks by saline solutions derived from associated evaporite sequences. Thus, Brown (1971) has suggested that the copper mineralization in the Nonesuch Shale of the White Pine deposit results from replacement of pre-existing iron sulfides by copper-rich solutions that migrated upward from the underlying Copper Harbor Conglomerate. Detailed arguments for and against the various theories, which incorporate almost every possibility between the two extremes, can be obtained from the relevant literature (e.g., Fleischer, Garlick, and Haldane, 1976; Bartholomé, 1974; Jung and Knitzschke, 1976; Brown, 1971; Sweeney, Binda, and Vaughan, 1991). There is little reason to suspect that all deposits of this group have the same origin, although it is worth noting that, in even the most apparently undisturbed ores of this type, an appreciation of the role of chemical transformation and replacement during diagenesis is growing (e.g., Turner, Vaughan, and Whitehouse, 1978; Vaughan et al., 1989).

10.9 COPPER-IRON-ZINC ASSEMBLAGES IN VOLCANIC ENVIRONMENTS

Mineralogy

Major Pyrite, sphalerite, chalcopyrite; in some examples, pyrrhotite or galena

Minor Bornite, tetrahedrite, electrum, arsenopyrite, marcasite, cubanite, bismuth, copper-lead-bismuth-silver-sulfosalts, cassiterite, plus many others in trace amounts

Mode of Occurrence Massive to disseminated stratiform sulfide ores in volcanic-sedimentary sequences ranging from ophiolite complexes (Cyprus-type deposits), felsic tuffs, lavas and subseafloor intrusions (Kuroko-type deposits), to mudstones and shales with little immediately associated, recognizable volcanic material (Besshi-type deposits).

Examples Kuroko- and Besshi-type deposits of Japan; Timmins, Ontario; Bathurst, New Brunswick; Sullivan, British Columbia; Flin-Flon, Manitoba-Saskatchewan; Noranda, Quebec; Mt. Lyell, Australia; Rio Tinto, Spain; Scandinavian Calidonides; Avoca, Ireland; Parys Mountain, Wales; Troodos Complex deposits, Cyprus; Bett's Cove, Newfoundland; Modern Red Sea and East Pacific Rise deposits.

10.9.1 Mineral Associations and Textures

The deposits range from ores in thick volcanic sequences, such as the Kuroko ores of Japan and ores directly associated with a volcanic vent (Vanna Levu, Fiji), to ores associated with ophiolite sequences (Cyprus; Bett's Cove, Newfoundland) to distal ores that are emplaced in dominantly sedimentary sequences (Besshi deposits of Japan) and sequences containing no recognizable volcanics (Sullivan, British Columbia). They thus grade into ores of the type described in Section 10.8. In spite of the different settings in which these ores are found, there are similarities among the ore types observed. Zoning within many of these deposits is recognizable, and three major ore types occur; the distribution of the primary minerals in the Kuroko ores is shown in Figures 10.23 and 10.24. Although the major ore types described in the following are those commonly observed in the Kuroko deposits, they appear in most or all of the ores of this class, with only minor variations. These ores, which appear to grade into the ores described in Section 10.8, have frequently been considered in terms of Cu-Pb-Zn ratios, as shown in Figure 10.25. Plimer (1978) has suggested that a trend in ore type from Cu-dominant to Zn-dominant to Zn-Pb-dominant corresponds to a progression in time and distance from the volcanic source (i.e., proximal to distal in nature). Jambor (1979) has enlarged on this theme and has proposed a classification of the Bathurst-area (Canada) deposits based on their established or assumed displacement from feeder conduits (proximal versus distal) and the position of sulfide crystallization (autochthonous versus allochthonous).

Although the ores of the volcanic deposits are members of a continuum, several specific ore types are observed most commonly; the following is a brief discussion of these ore types.

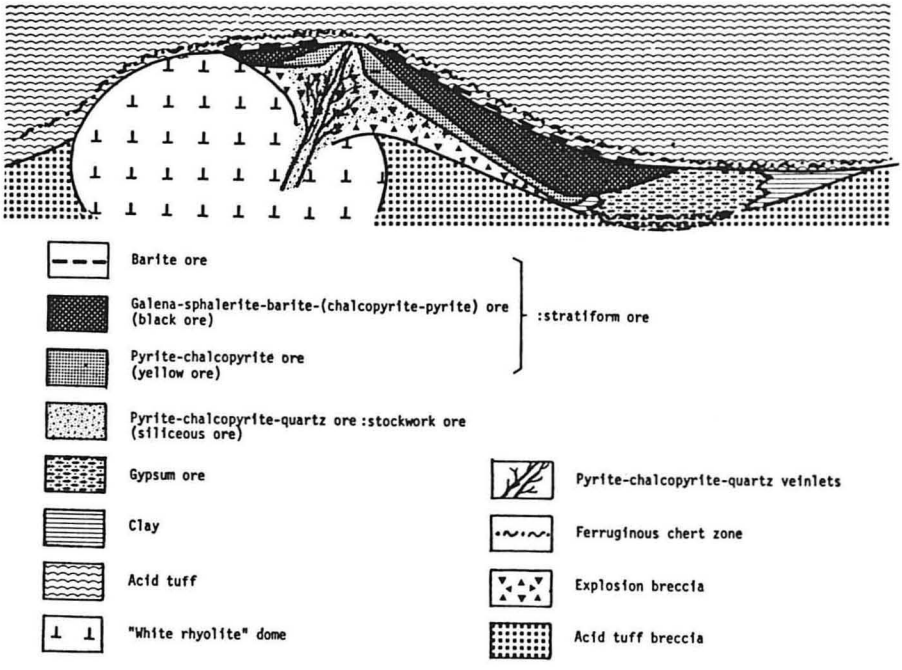

FIGURE 10.23 Schematic cross section of a typical Kuroko deposit. (From T. Sato, in *Geology of Kuroko Deposits*, Soc. Mining Geol. Japan, 1974, p. 2; used with permission.)

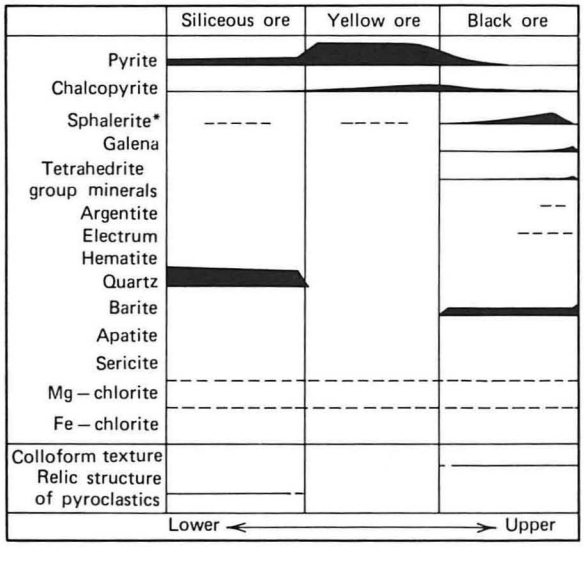

FIGURE 10.24 Distribution of major ore and gangue minerals in Kuroko-type deposits.

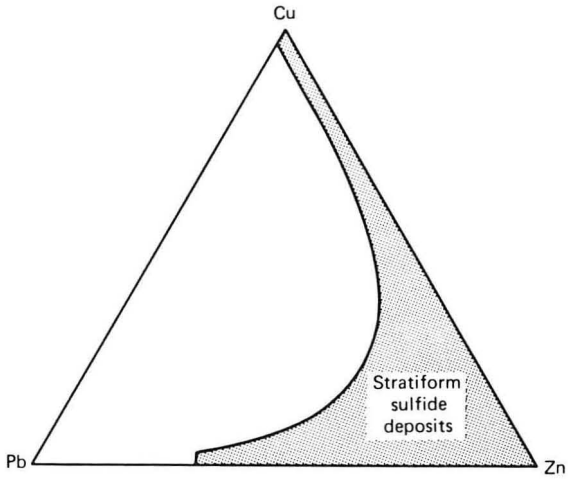

FIGURE 10.25 Plot of copper:lead:zinc ratios observed in stratiform sulfide ore deposits. A trend has been observed from copper to zinc to lead-zinc dominated ores with distance from the volcanic source.

Pyritic (or Cyprus Type) These types of ores, associated with ophiolite complexes, are composed of massive banded to fragmental pyrite with small amounts of interstitial chalcopyrite and other base-metal sulfides. The pyrite is present as friable masses of subhedral to euhedral, commonly zoned grains, as colloform banded masses, and as framboids. Marcasite is admixed with the pyrite and often appears to have replaced the pyrite. Chalcopyrite occurs as anhedral interstitial grains and as inclusions in the pyrite; sphalerite occurs similarly but is less abundant. Secondary covellite, digenite, chalcocite, and bornite occur as rims on, and along fractures, in pyrite and chalcopyrite.

Siliceous Ore (or Keiko Type of Kuroko Deposits) These types of ores apparently represent feeder veins and stockworks, and consist primarily of pyrite, chalcopyrite, and quartz, with only minor amounts of sphalerite, galena, and tetrahedrite. The pyrite occurs as euhedral grains, subhedral granular stringers, and colloform masses. The other minerals are minor and occur as anhedral interstitial grains in pyritic masses and gangue. Scott (personal commununication, 1980) has noted that a black siliceous ore composed of sphalerite and galena is not uncommon in Kuroko deposits.

Yellow Ore (or Oko Type of Kuroko Deposits) This ore type is characterized in both hand sample and polished section by the conspicuous yellow color resulting from the presence of chalcopyrite interstitial to the dominant euhedral to anhedral pyrite (Figure 10.26). Minor amounts of sphalerite, galena, tetrahedrite, and lead sulfosalts and trace amounts of electrum are dispersed among the major sulfides. In unmetamorphosed bodies, the pyrite is

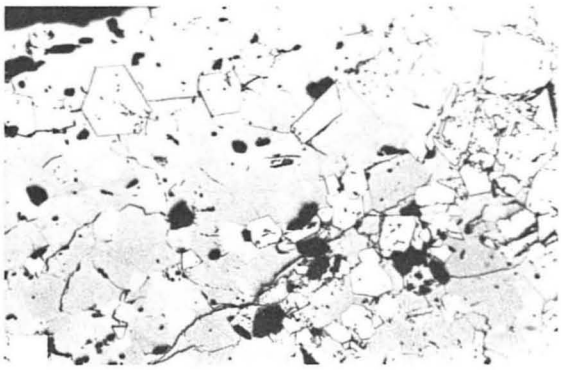

(*a*)

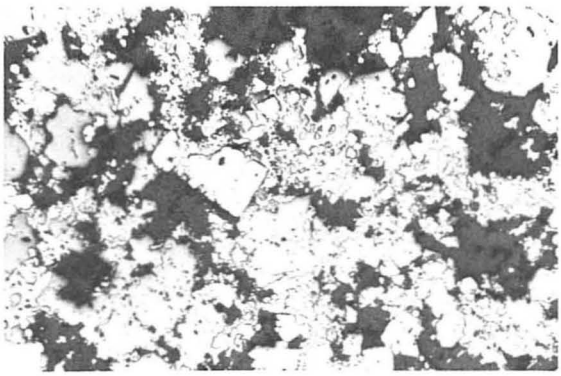

(*b*)

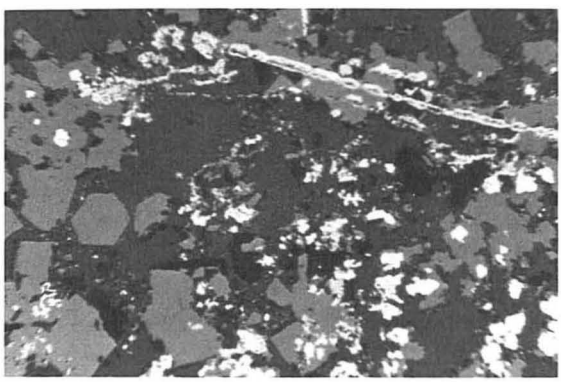

(*c*)

FIGURE 10.26 Typical Kuroko-type ores. (*a*) Yellow ore composed of euhedral pyrite crystals within a matrix of chalcopyrite, Ainai Mine, Japan (width of field = 2,000 μm). (*b*) Black ore composed of a matrix of irregularly intergrown sphalerite and galena containing euhedral and anhedral grains of pyrite, Furutobe Mine, Japan (width of field = 2,000 μm). (*c*) Midocean ridge "black smoker" deposit composed of wurtzite-sphalerite (medium gray; note characteristic hexagonal wurtzite crystal shapes in some grains) and pyrite-marcasite (white laths, filaments, and grains) (width of field = 600 μm).

often quite fine-grained (<0.1 mm), but in metamorphosed ores, pyrite commonly recrystallizes to form euhedral grains that are several millimeters across. These ores, and the black ores described later, commonly exhibit extensively developed clastic textures that apparently formed at the time of ore deposition or immediately thereafter as a result of slumping.

Black Ore (Kuroko Type) The black ores (Figures 10.26 and 7.4c), the most complex of the common volcanogenic ore types, were so named because of the abundant dark sphalerite within them. Galena, barite, chalcopyrite, pyrite, and tetrahedrite are common but subsidiary to the sphalerite. Bornite, electrum, lead sulfosalts, argentite, and a variety of silver sulfosalts are customary accessory minerals. The black ores are usually compact and massive, but primary sedimentary banding is often visible and brecciated and colloform textures are not uncommon. In ores unmodified by metamorphism, pyrite occurs as framboids, rosettes, colloform bands, and dispersed euhedral to subhedral grains. Pyrite grain size increases during metamorphism, but growth zoning is often visible either after conventional polishing or after etching. In polished sections, sphalerite appears as anhedral grains that frequently contain dispersed micron-sized inclusions of chalcopyrite. Barton (1978) has shown, by using doubly polished thin sections in transmitted light (see Figure 2.9 and Figure 7.18), that this "chalcopyrite disease" consists of rods and thin vermicular, myrmekitic-like growths, probably formed through epitaxial growth or replacement. He has also shown the presence of growth-banding and overgrowth textures in sphalerite and tetrahedrite. During metamorphism, the sphalerite is commonly recrystallized and homogenized, and the dispersed chalcopyrite is concentrated as grains or rims along sphalerite grain-boundaries.

Barite Ore, Gypsum Ore (Sekkoko), and Ferruginous Chert (Tetsusekiei) These three zones are often present in the Japanese volcanogenic ores but are difficult to recognize in many older volcanogenic ores; frequently, they contain few ore minerals. The barite zone usually overlies the black ore and consists of stratified barite. The gypsum zone consists of gypsum and anhydrite, with minor amounts of pyrite, chalcopyrite, sphalerite, and galena. The uppermost part of many volcanogenic deposits is a complex mixture of tuff and cryptocrystalline quartz, containing chlorite, sericite, and pyrite and colored red by small amounts of flaky hematite.

The terminology used here (siliceous ore, black ore, etc.) was developed to describe the little altered Japanese Kuroko-type ores and thus does not apply without some modification to their metamorphosed equivalents of other parts of the world. Probably, the principal changes during metamorphism are the development of significant amounts by pyrrhotite and the modification of textures (see Section 10.10). Nevertheless, the same general ore types (e.g., pyrite with chalcopyrite; sphalerite, pyrite, galena, chalcopyrite) are encountered in many deposits.

Fluid inclusion studies (Roedder 1976) indicate that the ore-forming fluids were generally of low salinity (less than 5 wt % NaCl equivalent) and ranged in temperatures up to about 300°C.

10.9.2 Origin of the Ores

The ores considered in this section have been variously described as massive pyrite deposits related to volcanism, stratabound massive pyritic sulfide deposits, and stratiform sulfides of marine and marine-volcanic association (Stanton, 1972). Although the degree of volcanogenic affinity varies from ores within a volcanic vent (Vanua Levu, Fiji) to intercalation of ores with volcanic clastics and flows (Kuroko ores, Japan) to the occurrence of ores within dominantly terrigenous sediments (Besshi-type deposits, Japan; Sullivan, British Columbia), the origin of the ores appears to be related to submarine exhalative or hydrothermal activity associated with volcanism or seafloor fracture zones. Early views held that all or most of the ores accumulated as a result of a "snowfall" of very fine-grained sulfides that formed as hot solutions issued onto the seafloor, as observed in modern sulfide formation at the island of Volcano and along the crest of the East Pacific Rise (Francheteau et al., 1979). Ore breccia textures have been interpreted as resulting from steam explosions and soft sediment slumping. Barton (1978) has pointed out that it is difficult to envisage the maintenance of seafloor temperatures of 200–300°C (as indicated by fluid inclusion studies) over wide areas for periods of time that are long enough to allow the growth of coarse-grained, zoned sphalerites. He has suggested that at least some sulfide formation must have occurred beneath a crust, either by recrystallization of earlier primary syngenetic sulfide or by introduction of a hot, saline, hydrothermal fluid into a mass of fine-grained sulfide. Fracturing, healing of cracks, overgrowth, and breccia textures suggest that crystal growth continued episodically and was interspersed with periods of slumping, boiling, or explosive activity. The deeper-seated fracture-filling siliceous pyrite-chalcopyrite ores appear to have formed by precipitation from hydrothermal solutions in feeder zones.

10.10 OPAQUE MINERALS IN METAMORPHOSED MASSIVE SULFIDES

Mineralogy

Major	Pyrite, pyrrhotite (hexagonal and monoclinic forms), sphalerite, chalcopyrite, galena, tetrahedrite
Minor	Cubanite, marcasite, arsenopyrite, magnetite, ilmenite, mackinawite

Mode of Occurrence In regionally metamorphosed rocks, especially volcanic sequences, at moderate to high metamorphic grades.

Examples Ducktown, Tennessee; Ore Knob, North Carolina; Great Gossan Lead, Virginia: Flin Flon, Manitoba; Sullivan, British Columbia; Mt. Isa, Broken Hill, Australia; Skellefte District, Sweden; Sulitjelma and Røros, Norway.

10.10.1 Mineral Associations and Textures

Few metalliferous ores owe their existence to regional metamorphism, but countless massive sulfide ores have been significantly altered by metamorphic effects. The mineral associations in these ores are largely dependent on the original (premetamorphic) mineralogy, and the textures are dependent on the original structure and the extent of thermal and dynamic metamorphism. The macroscopic effects of regional metamorphism include a general coarsening of grain size, development of schistosity, drag folds, isoclinal folding with attenuation of fold limbs and thickening in hinges, rupturing of folds, brecciation, and boudinage. The same deformation features are seen on a smaller scale under the ore microscope (Figure 10.27a), but additional structural details and certain mineralogic changes may also be evident. Frequently during dynamic metamorphism, lath-like silicates, pyrite, and magnetite are locally fractured and ductile sulfides, especially galena, chalcopyrite, pyrrhotite, and sphalerite, are forced into the resulting relatively low-pressure areas (Figure 10.27b). In micaceous ores, the sulfides may be forced along the basal cleavage planes of mica crystals (Figure 10.27c). In contrast to the ductile sulfides, the more brittle sulfides, such as pyrite and arsenopyrite, deform by fracturing and thus may be observed as shattered crystals, infilled by more ductile sulfides, or even as drawn out, lens-like polycrystalline aggregates. The effects of stress may be evident in the development of twinning (especially if twins are deformed), curved-cleavage traces (especially visible in galena), kinkbanding, undulose extinction (see Figures 7.20a, 7.20c, 7.22), and the presence of curved rows of crystallographically oriented inclusions (e.g., chalcopyrite in sphalerite). In pyrite, mild strain effects, such as the development of micromosaic structures, invisible after normal polishing, may be brought out by etching (conc. HNO_3 followed by brief exposure to 6M HCl).

Thermal metamorphism, even of ores that have previously or synchronously undergone intense deformation, commonly results in an increase in grain size and the development of 120° triple junctions in monomineralic masses. If small amounts of other phases are present, recrystallization may result in the entrapment of small lens-like grains that outline original grain boundaries (Figure 10.27d). In heterogeneous iron-sulfide-bearing ores, pyrite tends to recrystallize as euhedral cubic porphyroblasts, whereas chalcopyrite, pyrrhotite, and sphalerite tend to develop equant anhedral forms. Careful analysis of pyrite crystals often reveals that they possess growth zoning defined by inclusions of silicates, oxides, or other sulfides, as shown in Figures 7.28, 7.29, and 7.30. In dominantly iron sulfide ores, pyrite porphyroblasts are commonly 1 cm across but may, in extreme cases, reach 10–20 cm across (e.g., Ducktown, Tennessee; Grøsli, Norway) (see Figure 7.27).

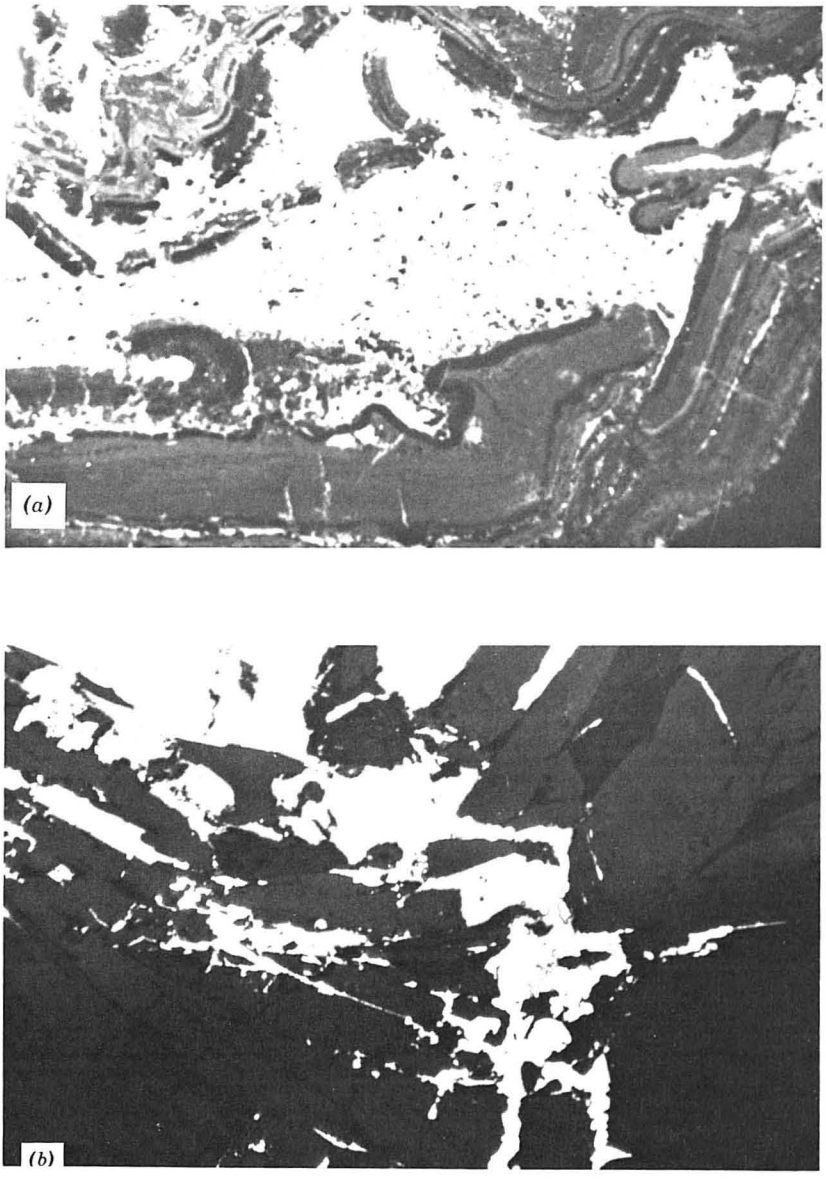

FIGURE 10.27 Textures observed in metamorphosed massive sulfides. (*a*) Severe distortion and disaggregation of primary banding in interlayered sphalerite (medium gray) and galena (white), Mt. Isa, Australia (width of field = 8 cm). (*b*) chalcopyrite (white) and sphalerite (light gray) injected into fractured amphiboles, Great Gossan Lead, Virginia (width of field = 700 μm). (From Henry et al., *Econ. Geol.* **74**, 651, 1979; used with permission). (*c*) Pyrrhotite injected along cleavages in a deformed biotite, Great Gossan Lead, Virginia (width of field = 400 μm). (*d*) Lens-like inclusions of galena defining the grain boundaries of recrystallized pyrite, Mineral District, Virginia (width of field = 520 μm).

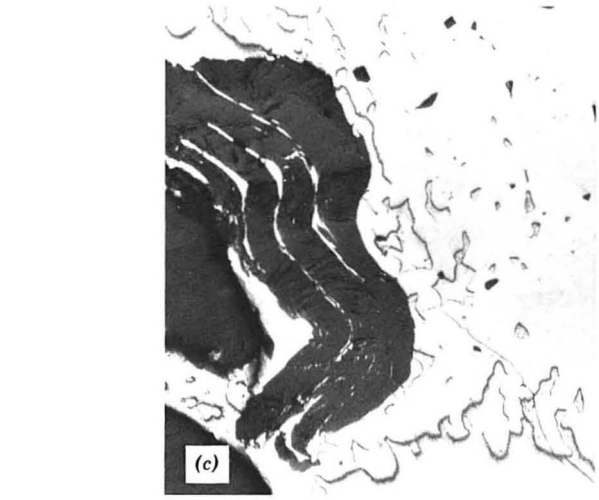

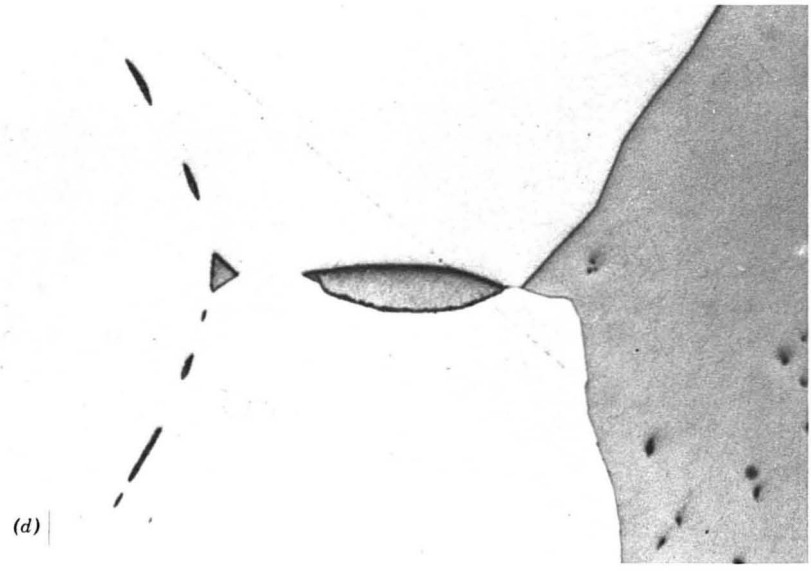

FIGURE 10.27 (*Continued*)

Mineralogic changes in sulfide ores depend on the grade of metamorphism. At lower grades, the more refractory sulfides (pyrite, sphalerite, arsenopyrite) tend to retain their original compositions and structures, while softer sulfides (chalcopyrite, pyrrhotite, and galena) readily recrystallize. However, at moderate to high grades, pyrite often begins to lose sulfur and be converted to pyrrhotite (see Section 7.7), and both pyrite and pyrrhotite may undergo oxidation to magnetite. Chalcopyrite commonly exhibits the development of laths of cubanite and very fine (~1 μm) wormlike inclusions of

mackinawite. Sphalerite and tetrahedrite, which retain original zoning at low grades of metamorphism, are homogenized at higher grades and tend to be brought into equilibrium with adjacent iron sulfides. The FeS content of sphalerite coexisting with pyrite and pyrrhotite, which varies as a function of pressure, has been calibrated as a geobarometer (Figure 10.28). To employ this geobarometer, the temperature of metamorphism must be determined by some independent means (e.g., fluid inclusions, trace element, or isotope partitioning). Sphalerites in metamorphosed ores commonly contain rows of small (< 5 μm) inclusions of chalcopyrite that appear to be the remnants of "chalcopyrite disease," primary depositional intergrowths. During recrystallization, the small chalcopyrite inclusions tend to concentrate and coalesce along grain boundaries. Experimental studies (Hutchison and Scott, 1981)

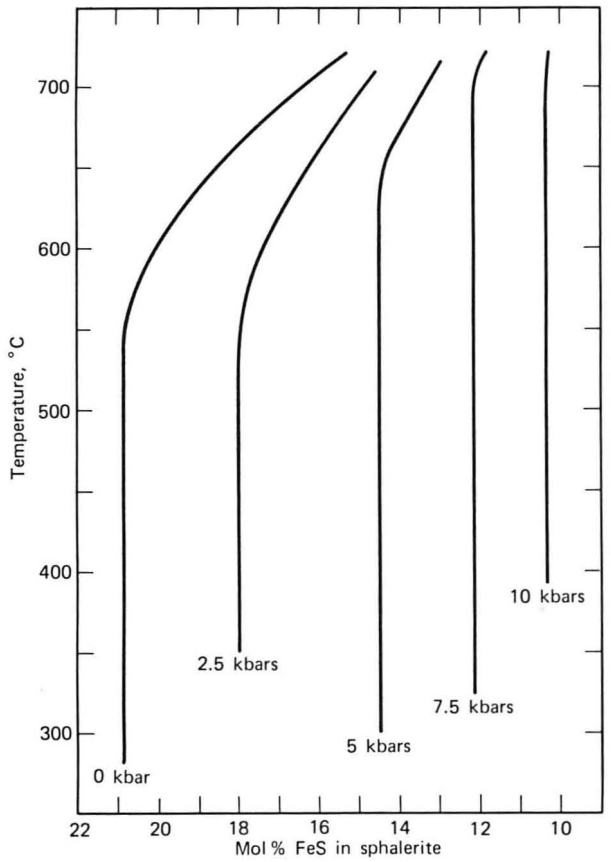

FIGURE 10.28 Plot of the FeS content of sphalerite coexisting with pyrite and hexagonal pyrrhotite at 0, 2.5, 5, 7.5, and 10 kbars at temperatures from 300–700°C. (After S. D. Scott, *Amer. Min.*, **61**, 662, 1976; used with permission.)

have shown that the solubility of CuS in sphalerite is very small below 500°C; hence, chalcopyrite should have little effect on the application of the sphalerite geobarometer. Nevertheless, chalcopyrite-bearing sphalerites often yield anomalous pressure estimates, possibly because the presence of the copper promotes low-temperature re-equilibration, and should be avoided in geobarometric studies. Furthermore, Barton and Skinner (1979) have suggested that sphalerite re-equilibrates by outward diffusion of FeS more readily when in contact with pyrrhotite than with the more refractory pyrite during post-metamorphic cooling. As a result, sphalerites coexisting with pyrrhotite commonly have lost some FeS after the peak of metamorphism and also indicate higher than actual metamorphic pressures. Accordingly, in applying the sphalerite geobarometer, it is important that you

1. Use only sphalerite that would have coexisted with pyrite and pyrrhotite during metamorphism but that is now encapsulated in pyrite
2. Avoid grains that contain, or coexist with, chalcopyrite or pyrrhotite
3. Choose the most FeS-rich sphalerites as indicative of the pressure during metamorphism

Arsenopyrite, although not abundant in these ores, may be a useful indicator of temperature if it is equilibrated with pyrite and pyrrhotite or other aS_2-buffering assemblages (Kretschmar and Scott, 1976) (Figure 8.19). As with all geothermometers, it must be applied with caution, and other independent checks on temperature should be employed if possible.

10.10.2 Origin of the Textures

The textures of metamorphosed ores result mainly from the dynamic deformation and heating accompanying regional metamorphism (see Sections 7.6 and 7.7). In some localities, deformation is minimal and recrystallization is the dominant change. In zones of intense deformation, the mineralogical character of the ore may be a factor that contributes to the obliteration of pre-metamorphic features and to the development of chaotic textures. This is especially true of ores rich in pyrrhotite, chalcopyrite, and galena, all of which suffer dramatic loss of shearing strength as temperature rises (Figure 10.29). The extreme flow of such ores often results in disaggregation of primary banding, the tectonic incorporation of wall rock fragments in "ball textures" (Vokes, 1973), and total reorientation—durchbewegung—of any surviving original features, thus rendering paragenetic interpretation difficult or impossible.

Prograde metamorphism results in corrosion of pyrite as sulfur is removed to form pyrrhotite, but retrograde re-equilibration often reverses the process, with pyrites regrowing as euhedral crystals, as described in Section 7.7.

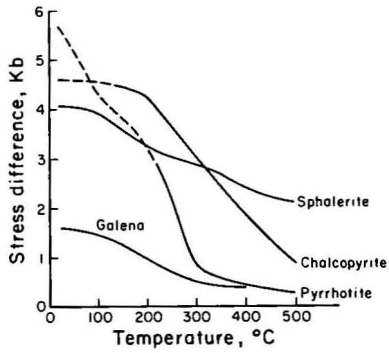

FIGURE 10.29 Shearing strength of some common sulfides as a function of temperature. (After W. C. Kelly and B. R. Clark, *Econ. Geol.* **70**, 431, 1975; reproduced with permission of the publisher.)

10.11 SKARN DEPOSITS

Mineralogy The mineralogy of skarn deposits varies widely; hence, generalizations should be regarded with caution. This discussion is confined to skarns that are important as sources of iron, molybdenum, tungsten, copper, lead, zinc, and tin and makes no attempt to treat the more unusual occurrences. Skarns have been classified in several ways, but Einaudi, Meinert, and Newberry (1981) in a comprehensive treatment note that the best basis is to use the dominant economic metal; they propose Fe, W, Cu, Zn-Pb, Mo, and Sn skarns. The economic viability of many skarns is based as much upon the gold content as on other metals; hence, many deposits originally classed as one of the types previously listed are now called goldskarns if they contain more than 1 g/ton Au (Meinert, 1989; Theodore, et al., 1991).

Major	(But highly variable from one deposit to another)—magnetite, molybdenite, sphalerite, galena, chalcopyrite, pyrrhotite, pyrite, aresenopyrite, wolframite, scheelite-powellite (fluorescent under UV light)
Minor	Pyrrhotite, cassiterite, hematite, gold, bismuth, silver-bismuth (-selenium) sulfosalts
Associated Minerals	Quartz, various garnets, amphiboles, pyroxenes, calc-silicates, olivines, talc, anhydrite (some phases fluorescent under UV light)

Mode of Occurrence Skarns (tactites) are composed dominantly of coarse-grained, commonly zoned calc-silicates, silicates and aluminosilicates, and associated sulfides and iron oxides. They form in high-temperature contact

metamorphic halos at the junction of intrusions and carbonate-rich rocks or, more rarely, Al- and Si-rich rocks. The occurrence of ore minerals in skarns ranges from massive iron oxides or sulfides in some deposits to disseminated grains and veinlets of sulfides, molybdates, and tungstates in others. Reaction skarns are narrow rims, often rich in Mn-silicates and carbonates, formed between an intrusion and carbonate-rich host rocks. Replacement skarns (ore skarns) are large areas of silicate replacement of carbonate rocks resulting from the passage of mineralizing solutions. These often contain appreciable amounts of Fe, Cu, Zn, W, and Mo.

Examples Battle Mountain (Au), Lower Fortitude (Au), Copper Canon (Cu), Nevada; Eagle Mountain (Fe), Darwin (Pb + Zn + Ag), Bishop (W + Mo + Cu), California; Twin Buttes (Cu), Christmas (Cu), Arizona; Hanover (Pb + Zn), Magdalena (Pb + Zn), New Mexico; Cotopaxi (Cu + Pb + Zn), Colorado; Cornwall and Morgantown (Fe), Pennsylvania; Iron Springs (Fe), Carr Fork (Cu), Utah; Lost Creek (W), Montana; Gaspé Copper (Cu), Murdockville (Cu), Quebec; Kamioka (Zn), Nakatatsa (Zn), Kamaishi (Fe + Cu), Chichibu (Fe + Cu + Zn), Mitate (Sn), Japan; Renison Bell (Sn), Tasmania; King Island, Australia.

10.11.1 Mineral Associations and Textures

Skarn deposits are typified by compositional banding, an abundance of garnets and calc-silicate minerals, and a wide variation in grain size. The garnets and calc-silicates are often poikiloblastic, with enclosed pyroxenes and ore minerals. The thickness of compositional bands and the size of mineralized areas vary from a few millimeters to hundreds of meters, depending on the nature of the intrusion and its fluid content and the type of host rock. In tungsten-bearing skarns, such as that in Bishop, California, the ore minerals occur as tiny inclusions, grain coatings, narrow veinlets, and occasionally as irregular polycrystalline aggregates up to 10 cm across. Sulfides occurring as disseminated grains (Figure 10.30a) and vein fillings are apparently late in the paragenetic sequence and frequently display replacement textures.

In massive magnetite replacement bodies (Figure 10.30b), such as those at Cornwall and Morgantown, Pennsylvania, and Iron Springs, Utah, the ores commonly display a laminated texture of alternating fine- to coarse-grained anhedral magnetite, with greenish chlorite- and carbonate-rich bands seen even at the microscopic scale. Pyrite, commonly nickel- and cobalt-bearing, is present as irregular lenses and euhedral crystals. Irregular polycrystalline aggregates of chalcopyrite frequently display rims of secondary phases, such as bornite, digenite, and covellite.

Replacement zinc-lead ores such as those at Hanover, New Mexico, and Darwin, California, consist of fine- to coarse-grained anhedral sphalerite, galena, pyrite, and lesser amounts of other sulfides interspersed with calc-silicates, garnets, and feldspars. Rose and Burt (1979) have noted that ores

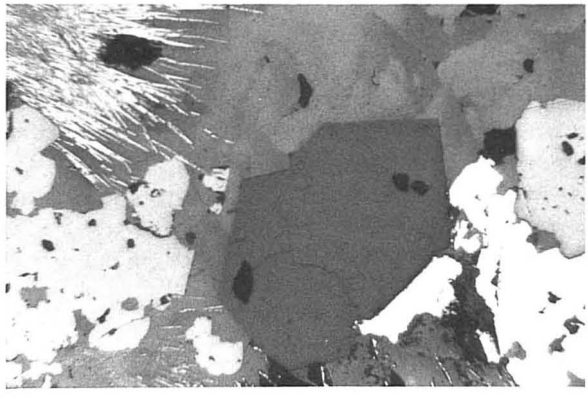

(a)

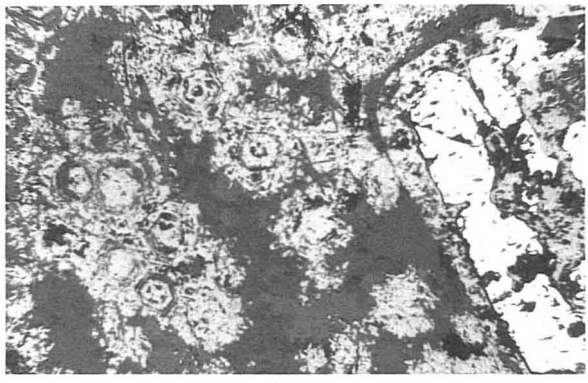

(b)

FIGURE 10.30 Typical skarn ores. (*a*) Grains of galena (white) and sphalerite (light gray) with sprays of hematite needles (note also the euhedral quartz crystals), Madan, Bulgaria (width of field = 1,200 μm). (*b*) Granular and concentrically growth-zoned magnetite and a portion of a pyrite crystal partially replaced by magnetite, Concepcion del Oro, Mexico (width of field = 1,200 μm).

often tend to be restricted to particular zones within the skarn, apparently as a result of (1) ground preparation, (2) skarn- and ore-forming solutions using the same "plumbing" systems, or (3) coprecipitation of some skarn and ore minerals.

10.11.2 Formation

Skarns form as zoned sequences along the contact of acid igneous intrusives with carbonates or more rarely Al + Si rich rocks (shales, gneisses) through the diffusion of hot reactive fluids. Burt (1974) has pointed out that the mineral zoning in many skarns can be explained by simple diffusion models that

assume simultaneous development of all major zones as a result of chemical potential gradients set up between dissimilar host rocks. Several types of diagrams, such as that presented in Figure 10.31, have been used to define the physico-chemical conditions under which the various zones have developed. Fluid inclusion and isotope studies, including those of skarn ores closely associated with porphyry-type deposits, indicate temperatures of formation from 225°C to more than 600°C and a considerable degree of interaction of hypersaline magmatic fluids with convecting ground water. Rose and Burt (1979) have summarized the genesis of a typical skarn deposit as occurring in the manner outlined as follows:

1. Shallow intrusion occurs of granitic (more rarely mafic) magma at 900–700°C into carbonate sediments.
2. Contact metamorphism at 700–500°C takes place with some reaction with, and recrystallization of, carbonates to form calc-silicates.
3. Metasomatism and iron-rich skarn formation at 600–400°C occur as a result of introduced magmatic and meteoric waters. The fluid properties change with time, becoming progressively enriched in sulfur and metals. The formation of skarn proceeds outward into the carbonate wall rocks

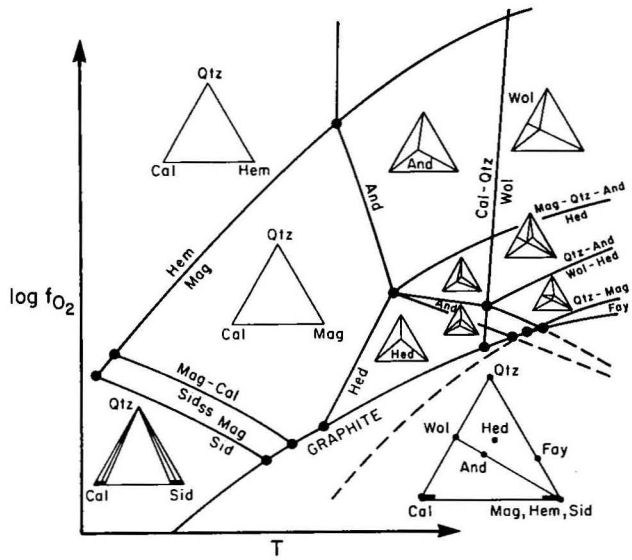

FIGURE 10.31 Schematic, low-pressure, isobaric log$f\,O_2$-T diagram for phases in equilibrium with vapor in the system Ca-Fe-Si-C-O. Abbreviations: cal, calcite; qtz, quartz, hem, hematite; sid, siderite; wol, wollastonite; and, andradite; hed, hedenbergite; fay, fayalite; mag, nagnetite. (Some phase equilibria in the system Ca-Fe-Si-C-O, Ann. Rept. Geophysical Lab.; after D. Burt, *Carnegie Institute Washington Yearbook*, Vol. 70, 1971, p. 181, reproduced with permission.)

(exoskarn) and, from the calcium acquired by the fluid, into the solidifying intrusion (endoskarn). Diffusion gradients result in the formation of a series of skarn alteration zones, but, as temperatures drop, skarn destruction may begin and the formation of replacement bodies of magnetite, siderite, silica, or sulfides occurs.

4. Superposition of oxides and sulfides at 500–300°C occurs, with the formation of scheelite and magnetite commonly preceding sulfides.
5. Late hydrothermal alteration at 400–200°C causes skarn destruction and the breakdown of garnet (to calcite, quartz, hematite, pyrite, epidote, chlorite), clinopyroxene (to calcite, fluorite, quartz, oxides, sulfides, etc.), and wollastonite (to calcite, quartz, fluorite).

Skarn deposits are commonly related to porphyry-type deposits (Section 9.5) and occur in carbonate beds adjacent to the intrusions. Skarns are also sometimes spatially and genetically related to the greisen (tin-tungsten-molybdenum-beryllium-bismuth-lithium-fluorine) type of mineralization that occurs locally adjacent to acid intrusives.

10.12 EXTRATERRESTRIAL MATERIALS: METEORITES AND LUNAR ROCKS

Mineralogy

Major	Troilite, kamacite, taenite, copper, schreibersite, ilmenite, chromite, cubanite
Minor	Graphite, cohenite, mackinawite, pentlandite, magnetite, daubréelite, alabandite, sphalerite, rutile, armalcolite $[Fe,Mg)Ti_2O_5]$ (lunar only)
Secondary	Goethite, lepidocrocite, maghemite, magnetite, pentlandite, pyrite

Mode of Occurrence Opaque minerals are present in nearly all meteorites, but the proportion is variable, ranging from 100% in some irons to only a few percent in some chondrites and achondrites where the opaque minerals are interstitial between olivine, orthopyroxene, and minor plagioclase. The lunar rocks and the soils contain many of the same opaque minerals, although as much as 75% of the opaques in the soils are considered to be of meteoritic origin.

Examples Meteorites are subdivided into four major groups, which in decreasing order of abundance are as follows: (1) chondrites (primarily silicates with visible chondrules), (2) irons (nearly all opaques), (3) achondrites (primarily silicates without chondrules), and (4) stony irons (roughly equal amounts of silicates and opaques). The many specimens studied appear to be fairly representative of the meteorite material in the solar system. The degree

to which our lunar samples reflect the composition of the moon's surface is uncertain; the similarity of specimens from distant localities is encouraging, but the number of samples is very limited.

10.12.1 Opaque Minerals in Meteorites

Although the relative amounts of opaque minerals in meteorites range from nearly 100% in irons to only a few percent in some chondrites and achondrites, the ore minerals that occur most abundantly in virtually all meteorites are kamacite, taenite, "plessite" (a fine intergrowth of kamacite and taenite), and troilite. Kamacite is α-iron, which contains a maximum of about 6% nickel. The iron meteorites with less than about 6% Ni, the hexahedrites, normally consist of large cubic (cube = hexahedron) crystals of kamacite. Cleavages and twinning are brought out as fine lines (Neumann lines or bands) by etching polished surfaces. Accessory minerals include grains of schreibersite, troilite, daubréelite, and graphite. With increasing nickel content (6–14%), the hexahedrites grade into octahedrites, the most common of iron meteorites. The octahedrites are so named because they show broad bands of kamacite bordered by taenite lamellae parallel to octahedral planes—the Widmanstätten structure (Figure 10.32). The iron-nickel phases are recognizable by their high reflectance, hardness, fine polish, and isotropism; kamacite is generally

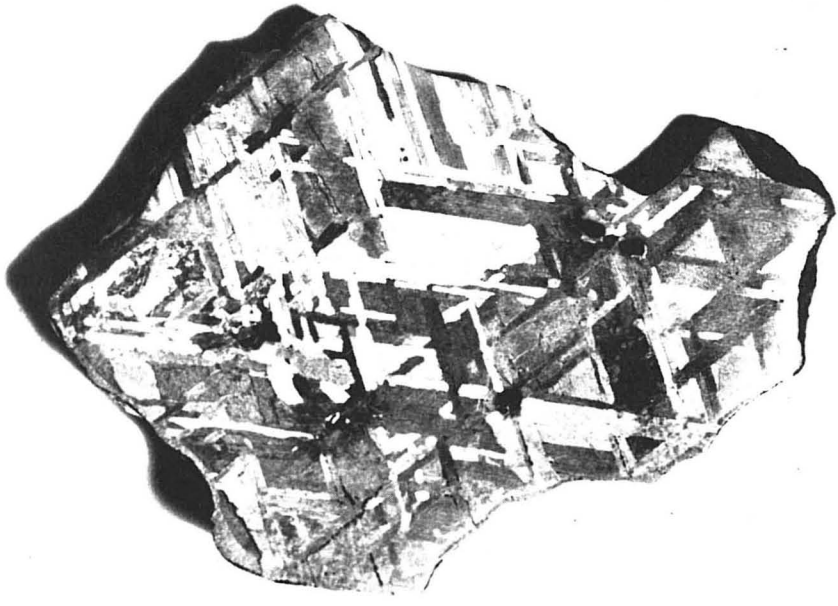

FIGURE 10.32 Widmanstätten structure in one of the Henbury, Australia, meteorites shown after etching. (Photograph courtesy of American Meteorite Laboratory, Denver, Colorado.)

light bluish gray, whereas taenite is white with a slight yellowish tint. Plessite is present in the angular interstices between bands, and accessory minerals present in minor amounts include schreibersite, troilite, copper, cohenite, mackinawite, grpahite, chromite, daubréelite, sphalerite, and alabandite.

In the stony meteorites, troilite, recognized by its pinkish brown color, moderate anisotropism, and lower reflectance and hardness than the alloys, is frequently as abundant as the iron phases (Figure 10.33a). It usually occurs as single phase and occasionally occurs as twinned anhedral grains, but intergrowths with pentlandite, daubréelite, and mackinawite are common.

Chromite is relatively common in small amounts and varies from euhedral crystals to myrmekitic intergrowths with silicates; ilmenite is occasionally present as exsolution lamellae. Other minor phases commonly associated with iron phases include copper, schreibersite, oldhamite (Ca,Mn)S, cohenite, and graphite (as a breakdown product of cohenite). Minor phases commonly associated with the troilite include daubréelite (as lamellae in troilite), pentlandite, mackinawite, niningerite (Mg,Fe,Mn)S, sphalerite, and chalcopyrite.

10.12.2 Secondary Minerals Resulting from Weathering of Meteorites

Meteorites, when exposed to the earth's atmosphere, undergo fairly rapid weathering, with the formation of secondary phases similar to those seen in terrestrial gossans. Kamacite, taenite, troilite, and schreibersite weather rapidly; chromite, ilmenite, and magnetite weather more slowly; and daubréelite weathers very slowly. The iron-bearing minerals are converted into a "limonite" (actually goethite and lepidocrocite) shell, with interspersed thin lenses of magnetite and maghemite (Figure 10.33b). Troilite is converted either to magnetite or locally to marcasite and pyrite. Secondary pentlandite forms when nickel released from the weathering of taenite and kamacite reacts with troilite.

10.12.3 Opaque Minerals in Lunar Rocks

The intense investigation of the retrieved lunar specimens has revealed a suite of opaque minerals that is very similar to that observed in meteorites. In fact, as much as 75% of the lunar opaques (and perhaps nearly 100% of those larger than 125 μm) ar estimated to be of an initial meteoritic origin from the impact of meteorites on the lunar surface. However, the distinction between original lunar and original meteoritic phases is not always clear. The four most abundant ore minerals in presumed primary lunar rocks are ilmenite, kamacite, taenite, and troilite (Figure 10.34). The best, but cautiously used, criterion for distinguishing lunar kamacite and taenite from that of meteoritic origin is the presence of much higher (0.8–3.0+%) cobalt contents and commonly lower nickel (<4%) contents of the former. The meteoritic kamacite and taenite are similar to those directly observed in meteorites, except that much of it has lost its original Widmanstätten structure as a result of shock or thermal meta-

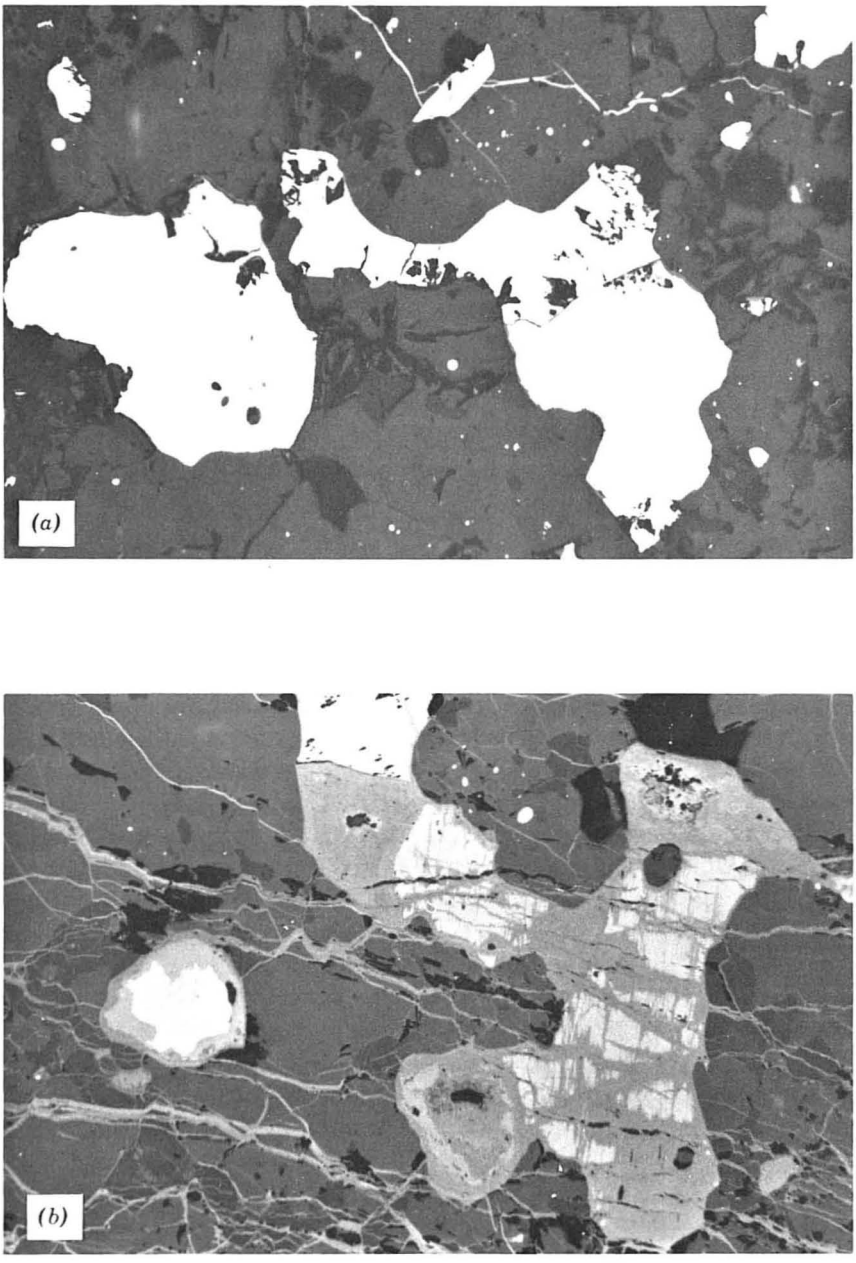

FIGURE 10.33 (*a*) Troilite (light gray) with native iron (white), Ashmore Meteorite, Texas (width of field = 520 μm). (*b*) Goethite (medium gray) produced by alteration of troilite (light gray), Ashmore Meteorite, Texas (width of field = 520 μm).

FIGURE 10.34 Opaque minerals in lunar rocks. (*a*) Native iron (white) in troilite surrounded by ilmenite (width of field = 520 μm). (*b*) Ilmenite rimmed by ulvöspinel with associated chromite and native iron (width of field = 520 μm). (NASA samples 70017, 224; 12002, 396, respectively.)

morphism. Presumed primary lunar iron occurs as dendrites, thin veinlets, needles, and tiny (< 5 μm) globules on silicates or on troilite. Much of this iron is interpreted as having formed as a reduction breakdown product of fayalite-rich olivines or primary iron-containing oxides.

Troilite is disseminated throughout the crystalline lunar rocks as subrounded interstitial grains, generally less than 50 μm across. It also occurs as thin veinlets in ilmenite and as spherules on the walls of small cavities. Its common association with iron suggests that it may have formed through the crystallization of an Fe-FeS melt that was immiscible in the silicate liquid. Optically, the lunar troilite is identical to the meteoritic material, but the former commonly contains less nickel and phosphorous than the latter.

Certain lunar rocks are relatively rich in titanium, which is present in a variety of oxide spinels but largely occurs as ilmenite, the most abundant lunar opaque mineral constituting as much as 20% by volume of some rocks. The ilmenite is present in various forms:

1. Blocky euhedral to subhedral crystals (< 100 μm) (Figure 10.34).
2. Thin, rhombohedral platelets parallel to (0001).
3. Coarse skeletal crystals (< 0.5 mm) intergrown with pyroxene, troilite, and iron. The blocky grains sometimes have cores or rims of armalcolite or chromian ulvöspinel (Figure 10.34). Lunar ilmenite, like terrestrial ilmenite, is tan colored, distinctly anisotropic, occasionally twinned, and may be translucent. Rutile is occasionally present as inclusions and lamellae within the ilmenite.

The oxide spinels are represented in the lunar rocks. They are rather variable in composition but can be described as members of two groups: (1) aluminous members of the chromite-ulvöspinel series or (2) chromian members of the hercynite-spinel series. The former are more numerous than the latter and occur in all lunar rock types as euhedral to subhedral grains in troilite, olivine, and pyroxene. Commonly, chromite cores have ulvöspinel rims. Reduction has frequently resulted in the formation of oriented laths of ilmenite and iron or a rim of ilmenite in which they are needles of iron. The hercynite-spinel minerals are rarer but are present as small euhedral to subhedral crystals (< 200 μm) in lunar basalts and peridotites. These minerals are reddish to pale brown in reflected light but red to orange in thin section.

Armalcolite, $(Fe,Mg)Ti_2O_5$, a lunar mineral related to terrestrial pseudobrookite and named for the three astronauts who first brought back lunar samples, occurs as small subhedral to euhedral grains coexisting with iron in fine-grained basalts. Frequently, it is rimmed or partly replaced by ilmenite.

Other opaque mineral phases that occur only rarely in lunar samples and that are commonly associated with the troilite as rims, along fractures, and as exsolution lamellae include copper, mackinawite, pentlandite, bornite, chalcopyrite, cubanite, sphalerite (15–25% Fe), and niningerite. Schreibersite and cohenite have been identified but are probably of meteoritic origin.

REFERENCES

Anderson, G. M. (1975). Precipitation of Mississippi Valley-type ores. *Econ. Geol.* **70**, 937–942.

_____. (1991). Organic maturation and ore precipitation in southeast Missouri. *Econ. Geol.* **86**, 909–926.

Anderson, G. M., and MacQueen, R. W. (1982). Mississippi Valley-type lead zinc deposits. *Geoscience Canada* **9**, 108–117.

Bartholomé, P., ed. (1974). Gisements stratiforms et provinces cupriferes. *Société* Geologique de Belgique, Liege.

Barton, P. B. (1978). Some ore textures involving sphalerite from the Furutobe Mine, Akita Prefecture, Japan. *Min. Geol. (Japan)* **28**, 293–300.

Barton, P. B., and Skinner, B. J. (1979). Sulfide mineral stabilities. In H. L. Barnes (ed.), *Geochemistry of Hydrothermal Ore Deposits*, 2nd ed. Wiley-Interscience, New York, pp. 278–403.

Beales, F. W., and Jackson, S. A. (1966). Precipitation of lead-zinc ores in carbonate reservoirs as illustrated by Pine Point orefield. *Trans. Inst. Min. Metall.* **B75**, 278–285.

Bjørlykke, A., and Sangster, D. F. (1981). An overview of sandstone-lead deposits and their relationship to red-bed copper and carbonate-hosted lead-zinc deposits. *Econ. Geol. 75th Anniv. Vol.*, 179–214.

Blain, C. F., and Andrew, R. L. (1977). Sulphide weathering and the evaluation of gossans in mineral exploration. *Mineral. Sci. Eng.* **9**, 119–150.

Blanchard, R. (1968). Interpretation of Leached Outcrops. Nevada Bureau of Mines, Bull. No. **66**, 196 pg.

Brown, A. (1971). Zoning in the White Pine copper deposit, Ontonagon County, Michigan. *Econ. Geol.* **66**, 543–573.

Brown, J. S. (1970). Mississippi Valley-type lead-zinc ores. *Mineral. Deposita* **5**, 103–119.

Brown, J. S., ed. (1967). Genesis of stratiform lead-zinc-barite-fluorite deposits: a symposium. *Econ. Geol. Monograph* 3.

Burns, R. G., ed. (1979). *Marine Minerals.* Mineral. Soc. Am. Short Course Notes, Vol. 6.

Burt, D. M. (1974a). *Metasomatic Zoning in Ca-Fe-Si Exoskarns, Geochemical Transport and Kinetics.* Carnegie Institute Wash. Pub. No. 634, 287–293.

Bustin, R.M., Cameron, A. R., Grieve, D. A., and Kalkreuth, W. D. (1983). *Coal Petrology: Its Principles, Methods and Applications.* Geol. Assoc. Canada Short Course Notes, Vol. 3, 230 pp.

Cronan, D. S. (1992). *Marine Minerals in Exclusive Economic Zones.* Chapman and Hall, London.

Derry, D. R. (1960). Evidence of the origin of the Blind River uranium deposits. *Econ. Geol.* **55**, 906–927.

Einaudi, M. T., Meinert, L. D., and Newberry, R. J. (1981). Skarn deposits. *Econ. Geol. 75th Anniv. Vol.*, 317–391.

Feather, C. E., and Koen, G. M. (1975). The mineralogy of the Witwatersrand reefs. *Mineral. Sci. Eng.* **7**, 189–224.

Fleischer, V. D., Garlick, W. G., and Haldane, R. (1976). Geology of the Zambian Copperbelt. In K. H. Wolf (ed.), *Handbook of Stratabound and Stratiform Ore Deposits*, Vol. 6. Elsevier, Amsterdam, pp. 223–352.

Francheteau, J., et al. (1979). Massive deep-sea sulphide ore deposits discovered on the East Pacific Rise. *Nature* **277**, 523–528.

Frimmel, H. E., le Roex, A. P., Knight, J., and Minter, W. E. L. (1993). A case study of the post-depositional alteration of the Witwatersrand Basal Reef gold placer. *Econ. Geol.* **88**, 249–265.

Glasby, G. P., ed. (1977). *Marine Manganese Deposits.* Elsevier Oceanography Series (15). Elsevier, Amsterdam (Note particularly articles by Cronan; Sorem and Fewkes; Burns and Burns).

Granger, H. C., and Warren, C. G. (1974). Zoning in the altered tongue associated with roll-type uranium deposits. In "Formation of Uranium Ore Deposits," Proceedings of the Symposium on the Formation of Uranium Ore Deposits, International Atomic Energy Agency, Vienna, pp. 185–200.

Hagni, R. D. (1976). Tri-State Ore Deposits: The Character of Their Host Rocks and Their Genesis. In K. H. Wolf (ed), *Handbook of Stratabound and Stratiform Ore Deposits*, Vol 6. Elsevier, Amsterdam, pp. 457–494.

Hagni, R. D., and Grawe, O. R. (1964). Mineral paragenesis in the Tri-state District, Missouri, Kansas, Oklahoma, *Econ. Geol.* **59**, 449–457.

Hagni, R. D., and Trancynger, T. C. (1977). Sequence of deposition of the ore minerals at the Magmont Mine, Viburnum Trend, Southeast Missouri. *Econ. Geol.* **72**, 451–463.

Hatch, J. R., Gluskoter, H. J., and Lindahl, P. C. (1976). Sphalerite in coals from the Illinois Basin. *Econ. Geol.* **71**, 613–624.

Henry, D. L., Craig, J. R., and Gilbert, M. C. (1979). Ore mineralogy of the Great Gossan Lead, Virginia. *Econ. Geol.* **74**, 645–656.

Heyl, A. V. (1969). Some aspects of genesis of zinc-lead-barite-fluorite deposits in the Mississippi Valley, U.S.A. *Trans. Am. Inst. Min. Metall. Eng.* **78**, B148–160.

Hutchinson, R. W., and Viljoen, R. D. (1986). Re-evaluation of gold source in Witwatersrand ores. *S. African J. Geol.* **91**, 157–173.

Hutchison, M. N., and Scott, S. D. (1981). Sphalerite geobarometry in the Cu-Fe-Zn-S system. *Econ. Geol.* **76**, 143–153.

International Committee for Coal Petrography (1975). *International Handbook for Coal Petrography*, 2 ed. Fluorescence microscopy and fluorescence photometry, 2nd supplement to 2nd edition.

Ixer, R. A., and Townley, R. (1979). The sulphide mineralogy and paragenesis of the South Pennine Orefield, England. *Mercian. Geol.* **7**, 51–63.

Ixer, R. A., and Vaughan, D. J. (1993). Lead-Zinc-Fluorite-Baryte Deposits of the Pennines, North Wales and the Mendips. In R. A. D. Pattrick and D. A. Polya (eds.), *Mineralization in the British Isles.* Chapman and Hall, London.

Jambor, J. L. (1979). Mineralogical evaluation of proximal-distal features in New Brunswick massive-sulfide deposits. *Can. Mineral.* **17**, 649–664.

James, H. L. (1954). Sedimentary facies of iron formation. *Econ. Geol.* **49**, 235–293.

_____. (1966). Chemistry of the iron-rich sedimentary rocks. U.S. Geol. Surv. Prof. Paper No. 440.

Jung, W., and Knitzschke, G. (1976). Kupferschiefer in the German Democratic Re-

public (GDR) with Special Reference to the Kupferschiefer Deposit in the Southeast Harz Foreland. In K. H. Wolf (ed.), *Handbook of Stratabound and Stratiform Ore Deposits*, Vol. 6. Elsevier, Amsterdam, pp. 353–406.

Kelly, W. C., and Clark, B. R. (1975). Sulfide deformation studies: III experimental deformation of chalcopyrite to 2000 bars and 500°C. *Econ. Geol.* **70**, 431–453.

Kimberley, M. M., ed. (1978). *Uranium Deposits, Their Mineralogy and Origin.* Mineral. Assoc. Canada Short Course Hdbk, Vol. 3, Toronto.

Kretschmar, U., and Scott, S. D. (1976). Phase relations involving arsenopyrite in the system Fe-As-S and their application. *Can. Mineral.* **14**, 364–386.

Krumbein, W. C., and Garrels, R. M. (1952). Origin and classification of chemical sediments in terms of pH and oxidation-reduction potentials. *J. Geol.* **60**, 1–33.

Langmuir, D. (1978). Uranium solution-mineral equilibria at low temperatures with applications to sedimentary ore deposits in M. M. Kimberley (ed.), *Uranium Deposits, Their Mineralogy and Origin*, Min. Assoc. Canada Short course Handbook 3, Toronto, 14–55.

Marmont, S. (1987). Unconformity-type uranium deposits. *Geoscience Canada*, **14**, 219–229.

Meinert, L. D. (1989). Gold skarn deposits—geology and exploration criteria. In R. R. Keys, W. D. H. Ramsey, and D. I. Groves (eds.), *The Geology of Gold Deposits: The Perspectives in 1988. Econ. Geol. Monogr.* **6**, 537–552.

Minter, W. E. L. (1978). A sedimentological synthesis of placer gold, uranium and pyrite concentrations in Proterozoic Witwatersrand sediments. In A. D. Maill (ed.), *Fluvial Sedimentology*, Can. Soc. Petrol. Geol. Mem. **5**, 801–829.

_____. (1990). Paleoplacers of the Witwatersrand basin. *Mining Engin.* (February 1990), 195–199.

_____. (1991). Ancient placer gold deposits. In R. P. Foster (ed.), *Gold Metallogeny and Exploration*, Blackie and Son Ltd., London, pp. 283–308.

Minter, W. E. L., Goedhart, M., Knight, J., and Frimmel, H. E. (1993). Morphology of Witwatersrand gold grains from the Basal Reef: evidence for their detrital origin. *Econ. Geol.* **88**, 237–248.

Philips, G. N., and Myers, R. E. (1989). The Witwatersrand gold fields: Part II. An origin for the Witwatersrand gold during metamorphism and associated alteration, R. R. Keays et al., eds. The Geology of Gold Deposits: The Perspective in 1988. *Econ. Geol. Monogr.* **6**, 598–608.

Plimer, I. R. (1978). Proximal and distal stratabound ore deposits. *Mineral. Deposita* **13**, 345–353.

Pretorius, D. A. (1975). The depositional environment of the Witwatersrand goldfields: a chronological review of speculations and observations. *Mineral. Sci. Eng.* **7**, 18–47.

_____. (1976). The nature of the Witwatersrand gold-uranium deposits. In K. H. Wolf (ed.), *Handbook of Stratabound and Stratiform Ore Deposits*, Vol. 7. Elsevier, Amsterdam, pp. 29–88.

Price, F. T., and Shieh, Y. N. (1979). The distribution and isotopic composition of sulfur in coals from the Illinois Basin. *Econ. Geol.* **74**, 1445–1461.

Ramdohr, P. (1958). New observations on the ores of the Witwatersrand in South Africa and their genetic significance. *Trans. Geol. Soc. S. Afr.* **61**, 1–50.

Roedder, E. (1976). Fluid inclusion evidence on the genesis of ores in sedimentary and

volcanic rocks. In K. H. Wolf (ed.), *Handbook of Stratabound and Stratiform Ore Deposits*, Vol. 2. Elsevier, Amsterdam, pp. 67–110.

Rose, A. W. (1976). The effect of cuprous chloride complexes in the origin of red-bed copper and related deposits. *Econ. Geol.* **71**, 1036–1044.

Rose, A. W., and Burt, D. M. (1979). Hydrothermal alteration. In H. L. Barnes (ed.), *Geochemistry of Hydrothermal Ore Deposits*, 2nd ed. Wiley-Interscience, New York, pp. 173–235.

Sangster, D. F. (1976). Carbonate-Hosted Lead-Zinc Deposits. In K. H. Wolf (ed.), *Handbook of Stratabound and Stratiform Ore Deposits*, Vol. 6. Elsevier, Amsterdam, pp. 447–456.

Sato, T. (1974). Distribution and setting of the Kuroko deposits. *Soc. Mining Geol. Japan*, Spec. Issue 6, 1–10.

Scott, S. D. (1976). Application of the sphalerite geobarometer to regionally metamorphosed terrains. *Amer. Min.* **61**, 661–670.

Sorem, R. K., and Foster, A. R. (1972). Internal structure of manganese nodules and implications in beneficiation. In D. R. Horn (ed.), *Ferromanganese Deposits on the Ocean Floor.* NSF, Washington, D. C., pp. 167–179.

Stanton, R. L. (1972). *Ore Petrology.* McGraw-Hill, New York.

Sverjensky, D. A. (1986). Genesis of Mississippi Valley-type lead-zinc deposits. *Annual Rev. of Earth and Planet. Sci.* **14**, 177–199.

Sweeney, M. A., Binda, P. L., and Vaughan, D. J. (1991). Genesis of the ores of the Zambian Copperbelt. *Ore Geol. Reviews*, **6**, 51–76.

Theodore, T. G., Orris, G. J., Hammarstrom, J. M., and Bliss, J. D. (1991). Gold-bearing skarns. *U.S. Geol. Surv.* No. 1930 Bull. 61 pp.

Turner, P., Vaughan, D. J., and Whitehouse, K. I. (1978). Dolomitization and the mineralization of the Marl Slate (N.E. England). *Mineral. Deposita* **13**, 245–258.

Varentsov, I. M. (1964). *Sedimentary Manganese Ores.* Elsevier, Amsterdam.

Vaughan, D. J., and Ixer, R. A. (1980). Studies of the sulphide mineralogy of North Pennine ores and its contribution to genetic models. *Trans. Inst. Min. Metall.* **89**, B99–B109.

Vaughan, D. J., Sweeney, M., Freidrich, G., Diedel, R., and Haranczyk, C. (1989). The Kupferschiefer: an overview with an appraisal of the different types of mineralization. *Econ. Geol.* **84**, 1003–1027.

Vaughan, D. J., and Craig, J. R. (1978). Mineral Chemistry of Metal Sulfides. *Cambridge University Press*, Cambridge, 493 p.

Vokes, F. M. (1973). "Ball texture" in sulphide ores. *Geol. Foren. Stockholm Forh.* **195**, 403–406.

Young, T. P., and Taylor, W. E. G. (1989). *Phanerozoic Ironstones.* Spec. Pub. Geol. Soc. London **46**.

SUGGESTED READINGS

Atkinson, W. W., and Einaudi, M. T. (1978). Skarn formation and mineralization in the contact aureole at Carr Fork, Bingham, Utah. *Econ. Geol.* **73**, 1326–1365.

Basu, A., and Molinaroli, E. (1989). Provenance characteristics of detrital opaque Fe-Ti oxide minerals. *Jour. Sed. Petrol*, **59**, 922–934.

Baxter, J. L. (1977). Heavy Mineral sand deposits of Western Australia. *Geol. Surv. West. Aust. Miner. Resour. Bull.* **10**.

Boctor, N. Z., Kullerud, G., and Sweany, J. L. (1976). Sulfide minerals in Seelyville Coal III, Chinook Mine, Indiana. *Mineral. Deposita* **11**, 249–266.

Burns, V. M. (1979). Marine placer minerals. In Burns, R. G. (ed.), *Marine Minerals.* Min. Soc. Am. Short Course Notes, Vol. 6, 347–380.

Burt, D. M. (1974b). "Skarns in the United States—a review of recent research." IAGOD Working Group on Skarns, 1974 Meeting, Varna, Bulgaria.

Carpenter, R. H., and Carpenter, S. F. (1991). Heavy mineral deposits in the upper coastal plain of North Carolina and Virginia. *Econ. Geol.* **86**, 1657–1671.

Collins, B. I. (1977). Formation of scheelite-bearing and scheelite-barren skarns at Lost Creek, Pioneer Mountain, Montana. *Econ. Geol.* **72**, 1505–1523.

Collins, L. B., and Baxter, J. L. (1984). Heavy mineral-bearing strandline deposits associated with high-energy beach environments, southern Perth Basin, Western Australia. *Aust. Jour. Earth. Sci.* **31**, 287–292.

Constantinou, G., and Govett, G. J. S. (1973). Geology, geochemistry, and genesis of Cyprus sulfide deposits. *Econ. Geol.* **68**, 843–858.

Cox, D. P., and Theodore, T. G. (1986). Descriptive model of Cu skarn deposits. In D. P. Cox and D. A. Singer, *Ore Deposit Models, U.S. Geol. Soc. Bull.* **1693**, 86–87.

Craig, J. R., and Vokes, F. M. (1992). Ore Mineralogy of the Appalachian-Caledonian stratabound sulfide deposits. *Ore Geology Reviews*, **7**, 77–123.

Craig, J. R., and Vokes, F. M. (1993). The metamorphism of pyrite and pyritic ores: overview. *Mineral. Mag.* **57**, 3–18.

Dimanche, F., and Bartholome, P. (1976). The alteration of ilmenite in sediments. *Mineral. Sci. Engineer.* **8**, 187–201.

Economic Geology (1982). Vol. 77, No. 4, "A special issue devoted to skarn deposits."

Economic Geology (1993). Vol. 88, No. 8, "A special issue on sea-floor hydrothermal mineralization: New perspectives."

El Goresy, A. (1976). Oxide minerals in lunar rocks. In D. Rumble (ed.), *Oxide Minerals.* Mineral. Soc. Am. Short Course Notes, Vol. 3, p. EG-1-46.

_____. (1976). Oxide minerals in meteorites. In D. Rumble (ed.), *Oxide Minerals.* Mineral. Soc. Am. Short Course Notes, Vol. 3, p. EG-47-72.

Eldridge, C.S., Barton, P. B., and Ohmoto, H. (1983). Mineral textures and their bearing on formation of the Kuroko ore bodies. In H. Ohmoto and B. J. Skinner (eds.), Kuroko and Related Volcanogenic Massive Sulphide Deposits. *Econ. Geol. Monogr.* **5**, 241–281.

Fischer, R. P. (1968). The uranium and vanadium deposits of the Colorado Plateau region. In J. D. Ridge (ed.), *Ore Deposits of the United States*, 1933/67. A.I.M.E., New York, pp. 735–746.

Force, E. R. (1980). The provenance of rutile. *Jour. of Sed. Petrol.* **50**, 485–488.

_____. (1989). Geologic evolution of Trail Ridge eolian heavy-mineral sand and underlying peat, northern Florida. U.S. Geol. Surv. Prof. Paper No. 1499, 16 pp.

_____. (1991a). Geology of titanium-mineral deposits. Geol. Soc. Amer. Spec. Paper No. 259, 112 pp.

_____. (1991b). Placer deposits. In E. R. Force, J. J. Eidel, and J. B. Maynard (eds.), Sedimentary and diagenetic mineral deposits: a basin analysis approach to exploration. *Reviews in Economic Geology*, **5**, 131–140.

Franklin, J. M., Lydon, J. W., and Sangster, D. F. (1981). Volcanic-associated massive sulfide deposits. *Econ. Geol.* 75th Anniv. Vol., 485–627.

Frondel, J. W. (1975). *Lunar Mineralogy.* Wiley, New York.

Gluskoter, H. J. (1975). "Mineral matter and trace elements in coal." In Trace Elements in Fuel, Advances in Chemistry Series, No. 141, pp. 1–22.

_____. (1977). Inorganic sulfur in coal. *Energy Sources* **3**, 125–131.

Groen, J. L., Craig, J. R., and Rimstidt, J. D. (1990). Gold-rich rim formation on electrum grains in placers. *Canadian Mineral.* **28**, 207–228.

Hallbauer, D. K., and Utter, T. (1977). Geochemical and morphological characteristics of gold particles from recent river deposits and the fossil placers of the Witwatersrand. *Mineral. Deposita* **12**, 293–306.

Hutchison, C. S., ed. (1988). *Geology of Tin Deposits.* Springer-Verlag, Berlin, 718 pp.

Ishihara, S., ed. (1974). Geology of Kuroko deposits. *Soc. Min. Geol. Japan,* Special Issue No. 6.

Jowett, E. C. (1986). Genesis of Kupferschiefer Cu-Ag deposits by convective flow of Rotliegenede brines during Triassic rifting. *Econ. Geol.* **81**, 1823–1837.

Lambert, I. B., and Sato, T. (1974). The Kuroko and associated ore deposits of Japan: a review of their features and metallogenesis. *Econ. Geol.* **69**, 1215–1236.

Lawrence, L. J. (1973). Polymetamorphism of the sulphide ores of Broken Hill, N.S.W. Australia. *Mineral. Deposita* **8**, 211–236.

Levinson, A. A., and Taylor, S. R. (1971). *Moon Rocks and Minerals.* Pergamon, New York.

Lindsley, D. H. (1991). *Oxide Minerals: Petrologic and Magnetic Significance*, Vol. 25. Mineral Soc. Amer., Reviews in Mineralogy, p. 509, Washington, D.C.

Lydon, J. W. (1984). Volcanogenic massive sulphide deposits: Part I. A descriptive model. *Geoscience Canada* **11**, 195–202.

_____. (1988). Volcanogenic massive sulphide deposits: Part II. Genetic models. *Geoscience Canada* **15**, 43–65.

Mason, B. H. (1962). *Meteorites.* Wiley, New York.

Mason, B. H., and Melson, W. G. (1970). *The Lunar Rocks.* New York.

McDonald, J. A. (1967). Metamorphism and its effects on sulphide assemblages. *Mineral. Deposita* **2**, 200–220.

Mining Geology (Japan) (1978). Vol. 28, Nos. 4 and 5 are devoted to studies of Kuroko-type ores.

Mookherjee, A. (1976). Ores and metamorphism: temporal and genetic relationships. In K. H. Wolf (ed.), *Handbook of Stratabound and Stratiform Ore Deposits*, Vol. 4. Elsevier, Amsterdam, pp. 203–260.

Mucke, A., and Chaudhuri, J. N. B. (1991). The continuous alteration of ilmenite through pseudorutile to leucoxene. *Ore Geol. Rev.* **6**, 25–44.

Ohmoto, H., and Rye, R. O. (1974). Hydrogen and oxygen isotopic compositions of fluid inclusions in the Kuroko deposits, Japan. *Econ. Geol.* **69**, 947–953.

Ohmoto, H., and Skinner, B. J., eds. (1983). The Kuroko and related volcanogenic massive sulfide deposits. *Econ. Geol. Monogr.* **5**, 604 pp.

Perry, D. V. (1969). Skarn genesis at the Christmas Mine, Gila County, Arizona. *Econ. Geol.* **64**, 255–270.

Philips, G. N., Myers, R. E., Law, J. D. M., Bailey, A. C., Cadle, A. B., Beneke, S. D., and Giusti, L. (1989). The Witwatersrand gold fields: Part I, Postdepositional History, synsedimentary processes, and gold distribution, in R. R. Keays, et al., eds. The Geology of Gold Deposits: The Perspective in 1988. *Econ. Geol. Monogr.* **6**, 585–597.

Pirkle, E. C., and Yoho, W. H. (1979). The heavy mineral ore body of Trail Ridge, Florida. *Econ. Geol.* **65**, 17–30.

Precambrian iron-formations of the world. *Economic Geology* **68**:7(1973).

Ramdohr, P. (1973). *The Opaque Minerals in Stony Meteorites.* Elsevier, Amsterdam.

Rickard, D. T., and Zweifel, H. (1975). Genesis of Precambrian sulfide ores, Skellefte District, Sweden. *Econ. Geol.* **70**, 255–274.

Roy, S. (1968). Mineralogy of the different genetic types of manganese deposits. *Econ. Geol.* **63**, 760–786.

Scott, S. D. (1973). Experimental calibration of the sphalerite geobarometer. *Econ. Geol.* **68**, 466–474.

Scott, S. D., Both, R. A., and Kissin, S. A. (1977). Sulfide petrology of the Broken Hill region, New South Wales. *Econ. Geol.* **72**, 1410–1425.

Shepherd, M. S. (1990). Eneabba heavy mineral sand placers. In F. E. Hughes (ed.), *Geology of the Mineral Deposits of Australia and Papua, New Guinea*, Australia Inst. of Min. and Metal., Melbourne, pp. 1591–1594.

Shimazaki, H. (1980). Characteristics of skarn deposits and related acid magmatism in Japan. *Econ. Geol.* **75**, 173–183.

Shimazaki, Y. (1974). Ore minerals in the Kuroko-type deposits. In S. Ishihara (ed.), *Geology of Kuroko Deposits, Soc. Min. Geol. Japan*, Special Issue No. 6, 311–322.

Shoji, T. (1975). Role of temperature and CO_2 pressure in the formation of skarn and its bearing on mineralization. *Econ. Geol.* **70**, 739–749.

Smith, N. D., and Minter, W. E. L. (1980). Sedimentalogical controls of gold and uranium in two Witwatersrand paleoplacers. *Econ. Geol.* **75**, 1–14.

Stach, E., et al. (1975). *Coal Petrology*, 2nd ed. Gebrüder Borntraeger, Berlin.

Tatsumi, T., ed. (1970). *Volcanism and Ore Genesis.* University of Tokyo Press, Tokyo, Japan.

Vokes, F. M. (1969). A review of the metamorphism of sulphide deposits. *Earth Sci. Rev.* **5**, 99–143.

Woodward, L. A., Kaufman, W. H., Schumacher, O. L., and Talbott, L. W. (1974). Stratabound copper deposits in Triassic sandstone of Sierra Nacimiento, New Mexico. *Econ. Geol.* **69**, 108–120.

Zharikov, V. A. (1970). Skarns. *Int. Geol. Rev.* **12**, 541–559, 619–647, 760–775.